Torrefied Biomass Detoxification: Extended Residence Time Overcomes Heating Rate Effects on PCDD/PCDF Formation during Torrefaction

Łukasz Sobol [a,b,*] Juan A. Conesa [c,d] Dominika Sabat,[e] Paweł Telega,[b] Ireneusz Zawiślak,[f] Szymon Szufa,[g] and Arkadiusz Dyjakon [a]

** Corresponding author: lukasz.sobol@upwr.edu.pl*

DOI: 10.15376/biores.21.3.7074-7108

GRAPHICAL ABSTRACT

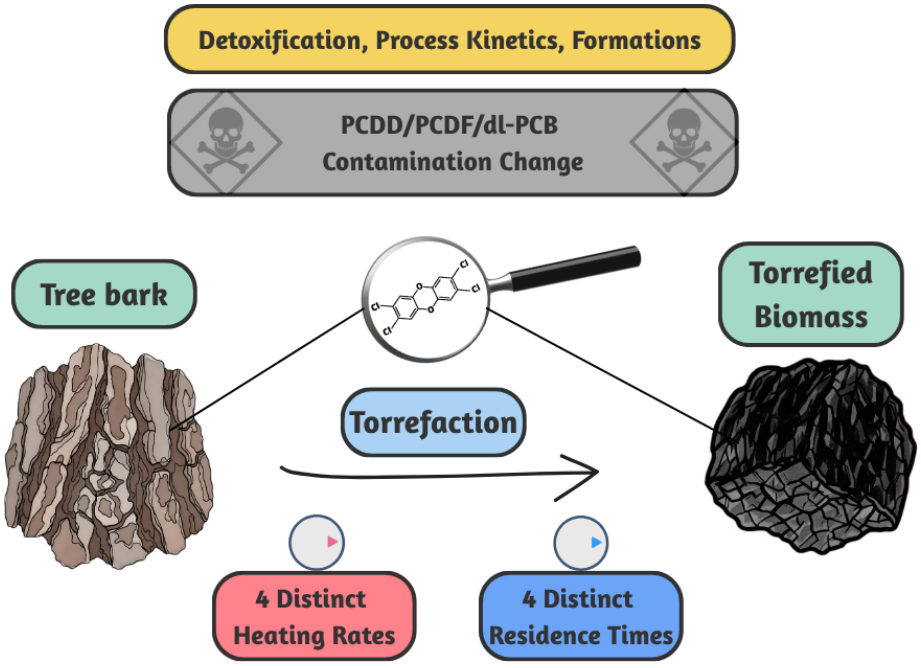

Torrefied Biomass Detoxification: Extended Residence Time Overcomes Heating Rate Effects on PCDD/PCDF Formation during Torrefaction

Łukasz Sobol [a,b,*] Juan A. Conesa [c,d] Dominika Sabat,[e] Paweł Telega,[b] Ireneusz Zawiślak,[f] Szymon Szufa,[g] and Arkadiusz Dyjakon [a]

Environmental applications of torrefied biomass may be severely limited by contamination with carcinogenic polychlorinated dibenzo-*p*-dioxins (PCDD), dibenzofurans (PCDF), and dioxin-like biphenyls (dl-PCB). In this article, the first systematic assessment of the influence of heating rate (HR) and residence time (RT) on the evolution of PCDD/PCDF/dl-PCB loads in bark-derived chars produced *via* torrefaction is presented. Sixteen torrefied biomass variants were examined, produced at a fixed temperature of 260 °C under different HR and RT conditions. Short processing durations (≤ 60 min) were found to induce a twofold increase in torrefied biomass toxicity (up to 1.314 ± 0.197 ng-TEQ·kg^{-1} 88% DM; DM stands for the dry matter), driven by precursor-mediated formation of PCDD/PCDF/dl-PCB, whereas extended residence times were shown to progressively detoxify the torrefied biomass, ultimately restoring toxicity levels comparable with, or markedly below, those of the raw biomass (0.689 ± 0.103 ng-TEQ·kg^{-1} 88% DM). The formation pathways of PCDD/PCDF/dl-PCB were governed by HR, as evidenced by the distinct kinetic profile observed at 30 °C·min^{-1}, reflecting suppression of the precursor-driven pathway, and by the newly identified "delay effect" of toxicity increase at 50 °C·min^{-1} conditions. Collectively, these findings demonstrate the critical influence of HR and RT on the optimization of torrefaction conditions to produce torrefied biomass with reduced PCDD/PCDF/dl-PCB contents.

DOI: 10.15376/biores.21.3.7074-7108

Keywords: Dechlorination; Torrefied biomass; Torrefaction; Dioxins; Detoxification; Kinetic parameters

*Contact information: a: Energy, Environment and Society Centre; Wrocław University of Environmental and Life Sciences, Grunwaldzki Square 24a, 50-363 Wrocław, Poland; b: Department of Applied Bioeconomy, Wrocław University of Environmental and Life Sciences, Chełmońskiego St. 37a, 51-630 Wrocław, Poland; c: Department of Chemical Engineering, University of Alicante, P.O. Box 99, E-03080 Alicante, Spain; d: Institute of Chemical Process Engineering, University of Alicante, P.O. Box 99, E-03080 Alicante, Spain; e: Faculty of Environmental Science and Technology, Wrocław University of Environmental and Life Sciences, 50-363, Wrocław, Poland; f: Department of Human Nutrition, Wrocław University of Environmental and Life Sciences, Chełmońskiego 37, 51-630 Wrocław, Poland; g: Faculty of Process and Environmental Engineering, Lodz University of Technology, Wolczanska, 213, 90-924, Lodz, Poland; *Corresponding author: lukasz.sobol@upwr.edu.pl*

INTRODUCTION

Polychlorinated dibenzo-*p*-dioxins (PCDD), dibenzofurans (PCDF), and dioxin-like biphenyls (dl-PCB) constitute a group collectively termed *dioxins*, which the Stockholm Convention classifies as persistent organic pollutants (UNEP 2001; Lacomba *et al*. 2025). Even at ultra-trace environmental concentrations, their lipophilicity drives

retention in fatty tissues, resulting in pronounced bioaccumulation and biomagnification throughout the food chain (Piskorska-Pliszczynska *et al*. 2014; García-Bermejo *et al*. 2017; Rao *et al*. 2022; Wang *et al*. 2024; Gülegen *et al*. 2025). The WHO highlights the extreme toxicity of dioxins, documenting their capacity to induce severe reproductive disorders, impair immune function, and disrupt endocrine regulation (WHO 2023). Moreover, the International Agency for Research on Cancer designates dioxins as carcinogenic to humans, thereby reinforcing global efforts to minimize potential exposure to the lowest levels (IARC 2012; Praud *et al*. 2025; Santa-Marina *et al*. 2026).

Dioxins occur ubiquitously across environmental matrices, including sewage, waste, water, soil, plants, and sediments (Rodriguez *et al*. 2008; Urbaniak and Zalewski 2011). While extensive knowledge exists regarding pollution levels, transport mechanisms, and mitigation strategies for most matrices, understanding dioxin contamination in biomass-derived chars, particularly that produced at relatively low temperatures, remains limited (Sobol *et al*. 2023). It represents a novel research area that has gained importance in recent years (Chen *et al*. 2021; Sobol *et al*. 2023, 2025b). This increased attention stems from findings that torrefied biomass may exhibit a higher PCDD/PCDF/dl-PCB toxicity load than the biomass feedstock (Gao *et al*. 2017; Sobol *et al*. 2024). Depending on the classification frameworks adopted by different authors, torrefaction is most commonly categorized as a thermochemical valorization process occurring within temperature ranges of 200 to 300 °C (*e.g*., Wang *et al*. 2017) or 200 to 320 °C (*e.g*., Sommersacher *et al.* 2018), or 200 to 350 °C (*e.g.*, Moscicki *et al.* 2014). Under the latter classification, torrefied biomass would formally abut with the classification of biochar production according to the new European Commission regulation, which employs the definition "at least 350 °C" (European Commission 2026), but not under the European Biochar Certificate, which applies the stricter criterion of "above 350 °C" (EBC 2012-2025a).

Although pyrolytic temperatures (≥450 °C), which are typical for biochar production, effectively volatilize/dechlorinate dioxins into non-toxic congeners (Grafmüller *et al*. 2024), such operating conditions are not always feasible due to (i) substantial economic costs of the process (Zhang *et al*. 2023a; Tripathi *et al*. 2024), as torrefaction requires less energy than high-temperature pyrolysis (Gonzales *et al*. 2025); (ii) intentional preservation of torrefaction-specific rather than biochar-specific physicochemical properties (Suthar *et al*. 2018). These findings challenge the suitability of torrefied biomass for prospective environmental applications, such as for soil (Chandrasekharan Nair *et al*. 2025) or for feed additives (Nair *et al*. 2023)—by raising concerns that it may release elevated levels of dioxins into the environment and, consequently, the food chain. In both cases, regulatory frameworks, especially in the EU, impose limits on PCDD/PCDF/dl-PCB concentrations to prevent potential risks to the environment and human health (BBodSchV Bundes-Bodenschutz- und Altlastenverordnung 1999; European-Union 2002; EBC 2012-2025a; Sobol *et al*. 2025b). This leads to a critical question of process design: how can biomass-derived material be produced through torrefaction to achieve environmental safety and increase the potential for future development of low-temperature materials? An interesting option may also be represented by the application of torrefaction as a pre-treatment step prior to pyrolysis. In the study by Han *et al*. (2021), the application of torrefaction before pyrolysis resulted in a 98.63% reduction in total dioxin content, including a 99.09% reduction of the toxic equivalent (TEQ) of volatile dioxins. This effect was attributed to the removal of 86.7% of HCl from the feedstock during torrefaction, which limited the chlorination of aromatic hydrocarbons and consequently reduced dioxin formation.

However, it was also observed that after the second stage (pyrolysis), the char produced from torrefaction-pretreated biomass exhibited higher toxicity than the char obtained by direct pyrolysis (Han *et al.* 2021). The development and optimization of torrefaction process parameters that could simultaneously enhance detoxification of the solid phase, leading to lower toxicity of the resulting char after the second stage, would contribute to achieving a more integrated and comprehensive process system.

In recent work (Sobol *et al*. 2025a), it was demonstrated that both temperature and the torrefaction process atmosphere (which may be inert (Růžičková *et al*. 2025), mildly-oxidative (Jindarom *et al*. 2006; Yang *et al*. 2018), and hydrothermal conditions (Jabeen *et al*. 2022)) govern the loading of PCDD/PCDF/dl-PCB in torrefied biomass. It was shown that, under inert and mildly-oxidative atmospheres, temperatures ≥280 °C promote effective detoxification of the torrefied biomass *via* preferential *meta*-position dechlorination of 2,3,7,8-substituted PCDD/PCDF congeners (Sobol *et al*. 2025a). Consequently, at 320 °C, the TEQ of torrefied biomass was reduced to nearly one order of magnitude below that of the raw biomass.

Although key mechanisms of PCDD/PCDF/dl-PCB formation across torrefaction temperatures were elucidated in that study (Sobol *et al*. 2025a), the experimental runs were intentionally structured with residence times (RT) sufficiently long to minimize kinetic constraints, while a constant, typical heating rate (HR) was applied. These parameters are frequently marginalized despite their decisive role in shaping the final toxicity of biomass-derived char. As demonstrated by Sobol *et al*. (2023), HR is often omitted from methodological descriptions, and PCDD/PCDF/dl-PCB toxicity is frequently not systematically assessed as a function of RT, even though research on other thermochemical processes has clearly established their substantial influence on dioxin formation dynamics (Addink and Altwicker 2004; Gao *et al*. 2016). In practice, pyrolytic toxicity-shift pathways are characterized by substantial complexity and are likely to involve multiple concurrent mechanisms (Sobol *et al*. 2025b). The current body of knowledge does not resolve whether, how, or to what extent control of RT and HR directs PCDD/PCDF/dl-PCB formation pathways and ultimately governs torrefied biomass toxicity. This uncertainty is particularly critical because the torrefaction window overlaps with the regime of heterogeneous dioxin formation mechanisms, including *de novo* synthesis (Zhang and Buekens 2016) and precursor-driven pathways (Altarawneh *et al*. 2009). These reactions are typically known to proceed between 200 and 400 °C on particle surfaces (ash/soot) and to be catalyzed by transition metals (*e.g.*, Cu/Fe/Zn) (Conesa and Mortes 2025).

In this study, the mechanisms governing dioxin formation across the torrefaction window were elucidated, and it was determined whether variations in HR and RT activate distinct PCDD/PCDF/dl-PCB formation/transformation pathways, thereby driving divergent trajectories of PCDD/PCDF/dl-PCB evolution. Furthermore, the role of controlled HR and RT modulation in driving PCDD/PCDF/dl-PCB detoxification was systematically evaluated. Ultimately, evidence-based guidance was provided on parameter ranges that should be avoided to prevent the production of torrefied biomass with elevated PCDD/PCDF/dl-PCB loads, which could increase the risk of transfer into the environment and the food chain.

MATERIALS AND METHODS

Feedstock and Initial Preparation

Mixed tree bark was selected as a model matrix for the experiment. The bark material was collected from the forest floor in a small, forested area located near Brzeg Dolny, in the vicinity of a town, chemical facility, industry manufacturing facilities, a high-traffic road, and residential households using individual heating systems. This sampling strategy was adopted to obtain biomass characterized by slightly elevated levels of PCDD/PCDF/dl-PCB compared to standard levels, thereby enabling a more mechanistic investigation of transformation pathways of these compounds during thermal processing and avoiding analytical limitations associated with concentrations below the limits of quantification (LOQ). The same bark matrix had been previously characterized and applied in earlier works (Sobol *et al*. 2025a,c), where details concerning species composition and geolocation of the sampling site were reported. For the present study, the bark was subjected to renewed comprehensive physicochemical characterization to ensure consistency with the experimental framework and to account for differences in research objectives, analytical scope, and methodological approaches.

Torrefaction necessitates that the raw material be pre-dried to a moisture content below 10% (Tumuluru *et al.* 2021). To meet this requirement, the biomass was accordingly dried at 105 °C for 24 h in a KBC-65 W drying chamber (WAMED, Warsaw, Poland). The dried bark was subsequently ground using an LMN 400 knife mill (TESTCHEM, Pszów, Poland), sieved to < 1 mm, and manually homogenized.

Torrefaction and Biomass Analyses

Torrefaction was performed in a muffle furnace (SNOL 8.2/1100, Uthena, Lithuania) at a fixed temperature of 260 °C under a continuous N_2 flow of 0.2 $L \cdot min^{-1}$. Four heating rates (HR: 5, 15, 30, and 50 $°C \cdot min^{-1}$) and four residence times (RT: 15, 60, 120, and 240 min) were systematically varied. Raw and torrefied biomass were characterized using ash/combustibles, ultimate, and metal content analyses. Photographs of the materials before and after torrefaction are provided in the Appendix (Figs. A2 and A3).

Ash content (AC) was determined using the gravimetric method by measuring the mass of the material before and after combustion in an SNOL 8.2/1100 muffle furnace (SNOL, Utena, Lithuania) according to the PN EN ISO 18122:2015. Combustible parts (CP) were expressed as material removed during the process. Moisture content (MC) was determined by an external laboratory in accordance with the method specified in Commission Regulation (EC) No 152/2009, Annex III, Part A. Mass loss (ML) was quantified gravimetrically by comparing the difference in sample weight before and after torrefaction.

The CHNS analysis was performed using a PerkinElmer 2400 Series II analyzer (Waltham, MA, USA). Metal analysis, following sample mineralization and dissolution, was conducted using a Varian SpectrAA 240FS instrument (Agilent Technologies, Santa Clara, CA, USA). Quantitative determination of Cr, Cd, Cu, Fe, Zn, and Mg elements was carried out by sequential atomic absorption spectroscopy, whereas quantitative determination of Na, K, and Ca was performed using flame atomic emission spectroscopy.

PCDD/PCDF/dl-PCB Determination

The analytical procedure used for PCDD/PCDF/PCB determination has been detailed in a previous publication (Sobol *et al*. 2025a). Briefly, analysis of 29 toxic PCDD/PCDF/dl-PCB congeners and 6 indicator ndl-PCB congeners (non-dioxin-like (ndl), sum of them referred to as ICES-6) was conducted by a commercial laboratory, J.S. Hamilton Poland. All measurements were performed in accordance with the laboratory's internal method PB-408 (3rd Ed., October 3, 2021). Results are reported in the form C ± U, where C denotes the concentration of the specified congener in the raw and torrefied biomass, and U represents the expanded measurement uncertainty (estimated for a expansion coefficient of k=2 and a 95% confidence level). LOQ are reported in Table 1. Regulatory frameworks typically require congeners with concentrations below the limit of detection to be assigned the LOQ value.

Table 1. LOQ for Specified PCDD/PCDF/dl-PCB and ndl-PCB Congeners

Group	Congener	LOQ
PCDD (ng/kg)	2,3,7,8-TCDD	0.05
	1,2,3,7,8-PeCDD	0.05
	1,2,3,4,7,8-HxCDD	0.05
	1,2,3,6,7,8-HxCDD	0.05
	1,2,3,7,8,9-HxCDD	0.05
	1,2,3,4,6,7,8-HpCDD	0.05
	OCDD	0.10
PCDF (ng/kg)	2,3,7,8-TCDF	0.05
	1,2,3,7,8-PeCDF	0.05
	2,3,4,7,8-PeCDF	0.05
	1,2,3,4,7,8-HxCDF	0.05
	1,2,3,6,7,8-HxCDF	0.05
	2,3,4,6,7,8-HxCDF	0.05
	1,2,3,7,8,9-HxCDF	0.05
	1,2,3,4,6,7,8-HpCDF	0.05
	1,2,3,4,7,8,9-HpCDF	0.05
	OCDF	0.10
dl-PCB (ng/kg)	PCB 077	0.05
	PCB 081	0.05
	PCB 126	0.05
	PCB 169	0.05
	PCB 105	10
	PCB 114	10
	PCB 118	10
	PCB 123	10
	PCB 156	10
	PCB 157	10
	PCB 167	10
	PCB 189	10
ndl-PCB (ug/kg)	PCB 028	0.10
	PCB 052	0.10
	PCB 101	0.10
	PCB 138	0.10
	PCB 153	0.10
	PCB 180	0.10

To obtain greater mechanistic insight, the authors elected not to apply this approach. Nevertheless, the concentrations of individual congeners provided in the Appendix enable TEQ values to be calculated using this or any alternative method, if required. A similar approach was also reported in a previous publication (Sobol *et al.* 2025a).

Statistical Analysis

To explore the relationships among torrefaction conditions, congener profiles, and TEQ values, principal component analysis (PCA) was applied, and a linear correlation coefficient heatmap was generated using Statistica 13 (TIBCO Software Inc.). Both analyses were conducted using a dataset based on LOQ/2 concentrations (concentrations of congeners falling below the detection limit were assumed to correspond to one-half of the LOQ). The PCA dataset comprised of 663 values, including the concentrations of 29 toxic PCDD/PCDF/dl-PCB, 6 ndl-PCB, and TEQ values for all scenarios (PCDD/PCDF, dl-PCB, PCDD/PCDF/dl-PCB, and ICES-6).

To provide additional mechanistic insight into PCDD/PCDF/dl-PCB formation, a kinetic model was developed in MATLAB (MathWorks), in which torrefaction was treated as a non-isothermal reactor system. The model evaluates three competing elementary pathways: (i) formation of dioxins from precursors (k_{form}); (ii) loss of precursors *via* evaporation/volatilization (k_{evap}); and (iii) detoxification *via* dechlorination of dioxins (k_{detox}). The process was mathematically described by a system of ordinary differential equations (ODEs) accounting for the dynamic temperature profile defined by the heating rate (HR). The ODE system was solved numerically using the finite-difference method. Kinetic parameters (pre-exponential factors and activation energies) were estimated by minimizing the sum of squared residuals between the experimental PCDD/PCDF/dl-PCB-TEQ values and the model predictions using the Nelder–Mead simplex algorithm. A complete mathematical description of the model, including all explicit equations, initial conditions, and assumptions, is detailed in Text A1 of the Appendix.

RESULTS AND DISCUSSION

Raw and Torrefied Biomass Characterization

Comprehensive physicochemical characteristics of the materials are presented in Table 2. As the metal content in the feedstock strongly influences the catalytic pathways of PCDD/PCDF formation (Cieplik *et al*. 2003; Cheruiyot *et al*. 2016; Themba *et al*. 2023), both transition metals (Cu, Cr, Cd, Fe, and Zn) and alkali and alkaline earth metals (Na, K, Ca, Mg) were evaluated. Markedly elevated Cr concentrations were observed in the tree bark (10.95 ± 0.19 $mg \cdot kg^{-1}$ DM), exceeding typical levels reported for plant tissues by more than an order of magnitude. Recent studies have demonstrated that this element alters the PCDD/PCDF signature (Zhang *et al*. 2023b). However, it should be acknowledged that the elevated level of this element could possibly be associated with steel abrasion occurring during bark grinding, because such risks may arise during biomass processing operations such as cutting (Mason *et al.* 2020). The concentrations of Na (19.83 ± 0.43 $g \cdot kg^{-1}$ DM) and Fe (294 ± 2 $mg \cdot kg^{-1}$ DM) were also exhibited moderate enrichments, whereas the remaining elements fell within ranges commonly reported for plants (Blum *et al*. 2009; Kirkby 2012).

Table 2. Characteristics of Raw and Torrefied Biomass

	Raw Biomass	HR5				HR15				HR30				HR50			
		RT15	RT60	RT120	RT240	RT15	RT60	RT120	RT240	RT15	RT60	RT120	RT240	RT15	RT60	RT120	RT240
AC (%)	6.26 ± 0.36	6.67 ± 0.12	7.53 ± 0.07	8.26 ± 0.24	9.37 ± 0.24	7.04 ± 0.10	8.73 ± 0.19	10.08 ± 0.12	11.27 ± 0.12	5.83 ± 0.08	7.88 ± 0.19	9.35 ± 0.08	9.58 ± 0.05	7.28 ± 0.06	8.80 ± 0.14	10.15 ± 0.25	10.41 ± 0.24
CP (%)	93.74 ± 0.36	93.33 ± 0.12	92.47 ± 0.07	91.74 ± 0.24	90.63 ± 0.24	92.96 ± 0.10	91.27 ± 0.19	89.92 ± 0.12	88.73 ± 0.12	94.17 ± 0.08	92.12 ± 0.19	90.65 ± 0.08	90.42 ± 0.05	92.72 ± 0.06	91.20 ± 0.14	89.86 ± 0.25	89.59 ± 0.24
MC* (%)	4.7 ± 0.3	1.3 ± 0.1	1.7 ± 0.1	1.2 ± 0.1	1.5 ± 0.1	1.7 ± 0.1	2.0 ± 0.1	1.7 ± 0.1	2.2 ± 0.2	2.7 ± 0.2	1.8 ± 0.1	1.1 ± 0.1	1.9 ± 0.1	2.8 ± 0.2	1.4 ± 0.1	2.0 ± 0.1	1.1 ± 0.1
ML (%)	---	4.78 ± 0.51	12.89 ± 1.26	18.45 ± 1.17	21.36 ± 1.28	2.17 ± 0.33	13.00 ± 1.25	18.79 ± 0.56	22.81 ± 0.98	3.02 ± 0.46	9.08 ± 0.97	20.93 ± 1.16	23.08 ± 1.02	1.02 ± 0.26	13.66 ± 1.42	19.14 ± 1.34	24.69 ± 0.92
C (%)	46.25 ± 0.50	51.11 ± 0.38	52.81 ± 0.45	55.86 ± 0.85	53.85 ± 1.28	49.39 ± 2.09	52.66 ± 2.91	54.21 ± 0.28	54.61 ± 0.62	47.10 ± 0.50	49.39 ± 1.45	53.31 ± 1.73	56.28 ± 0.73	46.93 ± 0.68	52.85 ± 1.53	54.36 ± 0.68	55.10 ± 0.77
H (%)	5.90 ± 0.11	5.82 ± 0.06	5.50 ± 0.11	5.44 ± 0.11	5.11 ± 0.23	5.83 ± 0.43	5.69 ± 0.35	5.58 ± 0.11	5.20 ± 0.13	5.41 ± 0.11	5.41 ± 0.13	5.33 ± 0.25	5.45 ± 0.10	5.60 ± 0.33	5.62 ± 0.16	5.10 ± 0.06	5.20 ± 0.04
N (%)	0.95 ± 0.06	0.76 ± 0.13	0.86 ± 0.13	0.95 ± 0.01	0.85 ± 0.03	0.93 ± 0.08	0.84 ± 0.09	1.00 ± 0.04	1.26 ± 0.06	0.95 ± 0.12	1.07 ± 0.01	0.94 ± 0.09	1.04 ± 0.02	0.89 ± 0.04	1.05 ± 0.04	1.11 ± 0.00	1.05 ± 0.11
S (%)	1.23 ± 0.08	1.46 ± 0.02	1.25 ± 0.33	1.39 ± 0.51	1.12 ± 0.04	1.29 ± 0.01	1.27 ± 0.15	1.26 ± 0.04	1.24 ± 0.23	1.28 ± 0.02	1.24 ± 0.22	1.10 ± 0.06	1.22 ± 0.14	1.44 ± 0.19	0.86 ± 0.35	1.21 ± 0.07	1.08 ± 0.11

Feedstock Metal Content									
Metal	Ca	Na	Mg	K	Cu	Cr	Cd	Fe	Zn
Unit	g/kg DM	mg/kg DM	g/kg DM	g/kg DM	mg/kg DM	mg/kg DM	mg/kg DM	mg/kg DM	mg/kg DM
Conc.	19.83 ± 0.43	47.04 ± 0.00	1.04 ± 0.01	1.70 ± 0.02	2.68 ± 0.10	10.95 ± 0.19	0.74 ± 0.04	294 ± 1.5	11.73 ± 0.08

AC, CP, C, H, N, S, Ca, Na, Mg, K were measured in 2 repetitions, ML was performed in 6 repetitions, Cr, Cd, Cu, Fe, Zn were measured in 4 repetitions. ± Represents SD, except for MC (measurement uncertainty). *MC results from analysis conducted by the J.S. Hamilton Laboratory for the determination of PCDD/PCDF concentrations.
Samples were delivered in dry form; therefore, the trace amounts of water detected reflect either inherent elemental moisture or water absorbed during transport and storage.

As expected, volatiles were removed during torrefaction, resulting in higher relative ash content in the torrefied biomass. Mass losses of up to 24.69 ± 0.92% were observed and were governed by the applied technological parameters. The proportional carbon content was increased, accompanied by a concomitant reduction in hydrogen content, reflecting progressive dehydration and devolatilization reactions (Zhang *et al*. 2025). For precise numerical values for each experimental variant, readers are referred to the Table 2.

Influence of HR and RT on TEQ, Concentration, and Profiles of PCDD/PCDF and dl-PCB

The evolution kinetics of TEQ (panels a–e) in torrefied biomass for PCDD/PCDF/PCB are illustrated in Fig. 1. Moderate PCDD/PCDF contamination was observed in the feedstock, with a concentration of 0.548 ± 0.082 ng-TEQ·kg^{-1} (88% DM). The TEQ profile was dominated by 2,3,7,8-TCDF, whereas OCDD accounted for the highest mass contribution (Figs. 2a-d). Overall, PCDF governed the toxicity profile of the feedstock, contributing nearly twice to the TEQ share compared to PCDD (65.67% *vs.* 34.33%). Detailed concentration data for all congeners in the feedstock and torrefied biomass are provided in the Appendix (Tables A1 to A5). Due to the low detection frequency of ndl-PCB, the authors elected to omit their discussion, as the available data provided limited scope for mechanistic interpretation. The evolution of ICES-6 concentrations in torrefied biomass, together with the concentrations of individual ndl-PCB congeners, is presented in the Appendix.

At a 15-min residence time (RT), lower heating rates (HR) were found to lead to the attainment of similar toxicity thresholds, resulting in more than a twofold increase in PCDD/PCDF concentrations and the corresponding TEQ values of 0.933 ± 0.140 ng-TEQ·kg^{-1} and 0.982 ± 0.147 ng-TEQ·kg^{-1} (88% DM) at HR of 5 and 15 °C·min^{-1}, respectively. *De novo* synthesis was effectively inhibited by maintaining an inert atmosphere in the chamber (Zhang and Buekens 2016), thereby ensuring that PCDD/PCDF formation primarily arises from precursor-mediated reactions involving chlorinated phenols and benzenes. This trend is evident for OCDD and OCDF (Figs. 2a,b), with a markedly larger increase observed in PCDD (27.5 → 79.7 ng·kg^{-1}) than in PCDF (8.9 → 16.2 ng·kg^{-1}) for the 5 °C·min^{-1} scenario (partial concentrations of congeners for which the concentration was below the LOQ were taken as LOQ/2 to express the sum of PCDD or PCDF concentrations). This pattern likely reflects the dominant role of chlorinated phenols as precursors, from which PCDD preferentially form (Nganai *et al*. 2014). However, the high LOQ in precursor analyses (chlorophenols/chlorobenzenes; Table A6 in Appendix) prevents full substantiation of this conclusion. Similar observations have been reported previously (Gao *et al*. 2017), where torrefaction was shown to initiate the precursor pathway, promoting PCDD formation from chlorinated phenols.

At an HR of 30 °C·min^{-1}, precursor-driven formation was observed to proceed less intensely. Although the qualitative pattern of change resembled that observed at slower HR, overall PCDD/PCDF formation remained lower, with TEQ increasing only to 0.743 ± 0.111 ng-TEQ·kg^{-1} (88% DM). In this specific HR, rapid heating promotes the early evaporation of solid-phase precursors, reducing the time they spend within the critical temperature window required for immediate catalytic reactions on the torrefied biomass surface. Notably, this HR does not reproduce the effect observed at 50 °C·min^{-1}, at which both PCDD/PCDF concentrations and TEQ remained essentially comparable to those of the feedstock. The rapid heating is considered to cause the sample to bypass the critical temperature window required for precursor condensation.

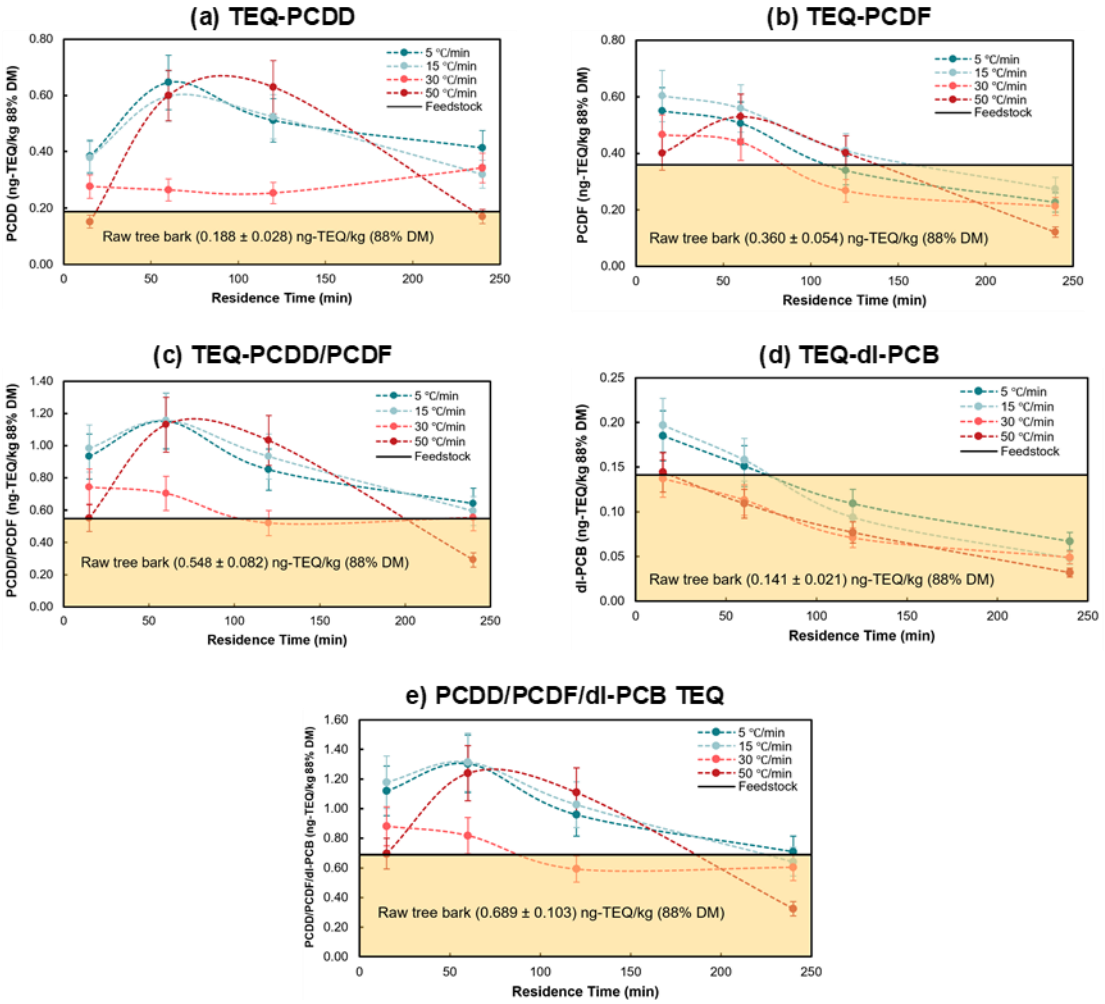

Fig. 1. (a–f) TEQ values of torrefied biomass (feedstock: bark, temperature: 260 ºC) depending on HR, RT and compound classification method; Panels plot data calculated using the LOQ/2 approach

From a technical perspective, readers should note that the black line representing the raw biomass level corresponds to the measured value without accounting for measurement uncertainty, which is provided separately in the figure as text. Accordingly, when measurement uncertainty is considered, this result does not appreciably differ from that of the raw biomass.

At an HR of 50 °C·min^{-1}, PCDD/PCDF formation exhibited a delayed start at 60 min (36.5 → 94.7 ng·kg^{-1}), with TEQ increasing to 1.130 ± 0.170 ng-TEQ·kg^{-1} (88% DM), whereas at slower HR, formation started earlier due to the prolonged residence of the biomass within the favorable temperature window. The kinetic model (Fig. 3d) confirms these observations. The physical delay observed at 50 °C·min^{-1} occurs because the rapid heating rate triggers a sudden generation of volatiles. This creates severe internal mass transfer limitations within the porous structure of the torrefied biomass. Consequently, the rate at which precursors are generated temporarily exceeds their ability to diffuse out of the pores. This extended residence time of precursors within the hot particle creates a highly favorable environment for the chemical formation pathway over physical

evaporation, explaining the pronounced, delayed spike in PCDD/PCDF formation at 60 minutes. Conversely, at 30 °C·min^{-1}, volatiles were allowed sufficient time to diffuse out of the torrefied biomass pores, consistent with the model prediction of lower toxicity at this HR compared with 50 °C·min^{-1}. These findings are in agreement with a previous report by Gao *et al*. (2016), in which it was demonstrated that high HR can decisively influence the selection of PCDD/PCDF formation pathways in a microwave-assisted process.

In contrast, when the residence time (RT) was extended to 60 min at slower HR (5 and 15 °C·min^{-1}), TEQ-PCDD/PCDF was further increased to 1.152 ± 0.173 and 1.156 ± 0.173 ng-TEQ·kg^{-1} (88% DM), respectively. This increase was attributed to a rise in TEQ-PCDD accompanied by a concurrent decline in TEQ-PCDF. The TEQ-PCDD was elevated as a result of *ortho*-dechlorination of OCDD and subsequent dechlorination of its transformation products, leading to increased concentrations of more toxic congeners, namely 1,2,3,6,7,8-HxCDD and 1,2,3,7,8-PeCDD (Figs. 2a,b), which are characterized by higher toxic equivalency factors (TEF) values. Conversely, the PCDF transformation was observed to proceed preferentially via *meta*-position dechlorination.

At an HR of 30 °C·min^{-1}, TEQ was altered only marginally, governed by concurrent *ortho*- and *meta*-dechlorinations of PCDD/PCDF. This process resulted in increased concentrations of 1,2,3,6,7,8-HxCDD and 1,2,3,7,8,9-HxCDD, while 1,2,3,7,8-PeCDD as well as 1,2,3,4,7,8-HxCDF, 1,2,3,6,7,8-HxCDF, and 2,3,4,7,8-PeCDF were reduced relative to the 15-min RT scenario. However, the developed kinetic model (Fig. 3d) was unable to reproduce the pronounced decline in TEQ, strongly indicating that physical transport limitations, particularly diffusion, play a key role.

These results are partially consistent with low-temperature fly ash experiments reported by Weber *et al*. (2002a; b), in which competitive dechlorination of OCDD at the *ortho* and *meta* positions was demonstrated. Furthermore, OCDF dechlorination was shown in their studies to proceed preferentially through *ortho*-position as the initial step, followed by *meta*-dechlorination. This behavior was partially observed in the present study under HR 15 °C·min^{-1}, as indicated by the increased formation of 1,2,3,4,6,7,8-HpCDF resulting from OCDF dechlorination.

Progressive extension of the RT was found to promote detoxification. However, the underlying mechanisms differed between HR. For HR of 5 and 15 °C·min^{-1}, extension of the RT beyond 60 min was observed to drive progressive dechlorination, occurring preferentially at the *meta*-position. After 240 min, TEQ decreased to levels comparable to those of the raw biomass (0.640 ± 0.096 and 0.594 ± 0.089 ng-TEQ·kg^{-1}, 88% DM, respectively). This behavior is fully consistent with a previous study (Sobol *et al*. 2025a), in which 90 min of torrefaction promoted *meta*-position dechlorination as the dominant detoxification mechanism, effectively suppressing the formation of toxic 2,3,7,8-substituted congeners.

At an HR of 30 °C·min^{-1}, further extension of RT largely reproduced the previously observed sequence of changes: TEQ decreased after 120 min and stabilized after 240 min, returning to a level comparable to that of the raw biomass (0.521 ± 0.078 and 0.555 ± 0.083 ng-TEQ·kg^{-1}, 88% DM, respectively). *Ortho*-dechlorination of OCDD and 1,2,3,4,6,7,8-HpCDD predominated, resulting in increased concentrations of 1,2,3,6,7,8-HxCDD (Fig. 2c). Notably, after 240 min, the concentration of 1,2,3,7,8-PeCDD was found to increase. In contrast, OCDF and toxic HpCDF underwent preferential *meta*-dechlorination, effectively reducing the toxic PCDF concentrations.

The behavior at a HR of 50 °C·min^{-1} differed slightly from that observed at slower HR. TEQ-PCDD/PCDF was observed to decrease gradually, although the dynamics and

trajectory of this decline were distinct. After 120 min, the concentrations of 1,2,3,7,8,9-HxCDD and 1,2,3,6,7,8-HxCDD were increased relative to the 60-min time point (Fig. 2d), due to double-cascade *ortho*-dechlorination of OCDD. In contrast, TEQ-PCDF decreased relative to the 60-min time point, thereby governing the overall trajectory of TEQ-PCDD/PCDF, primarily because of rapid *meta*-dechlorination of OCDF. In this variant, several congeners approached a pseudo-equilibrium state, indicating that their formation *via* dechlorination of higher-chlorinated congeners proceeded at rates comparable to those of subsequent decomposition/dechlorination. These observations support the presence of a complex equilibrium between *ortho*- and *meta*-dechlorination pathways rather than a single dominant mechanism.

After 240 min, degradation and *meta*-dechlorination were observed, resulting in a decrease of TEQ to values below those of the raw biomass (0.292 ± 0.044 ng-TEQ·kg^{-1}, 88% DM). These results establish RT as a key parameter controlling PCDD/PCDF detoxification in torrefied biomass, an effect that was previously proposed in pyrolysis (Hale *et al*. 2012) but not systematically evaluated. The kinetic model further confirms that the detoxification pathway dominates at prolonged RT in all cases, in agreement with the experimental observations.

In contrast, under shorter processing times, HR becomes an important parameter due to its influence on the pathways governing PCDD/PCDF and dl-PCB formation. Although literature values for chars derived from various thermochemical valorization processes are highly variable (Sobol *et al*. 2023), the TEQ levels determined for the torrefied biomass produced in this study may generally be regarded as being within the low-to-moderate range.

However, the classification of contamination levels as "low/moderate/medium/high" is inherently context-dependent and depends, *i.e.*, on the adopted reference framework, comparisons with specific char samples, or applicable regulatory threshold values. For a broader context, readers are referred to a previous review study (Sobol *et al*. 2023) in which over 100 char samples were systematically evaluated with respect to PCDD/PCDF contamination.

In the context of dl-PCB, similar effects of HR and RT were observed across all variants (Figs. 1d, 2a–d), except for the 15-min RT, where slower HR was found to induce a higher increase in TEQ-dl-PCB, which was likely due to enhanced formation through precursors. As the process progressed, dechlorination was observed to occur in the *meta* and *para* positions, effectively detoxifying the torrefied biomass and resulting in a substantial reduction of TEQ after 240 min. It should be noted, however, that from a reactor design perspective, a 4-h detoxification period poses substantial economic challenges when balancing safety requirements against process efficiency From a technical perspective, these two considerations can be balanced by maximizing the torrefaction residence time of the feedstock while accounting for the technical and economic constraints specific to each operator.

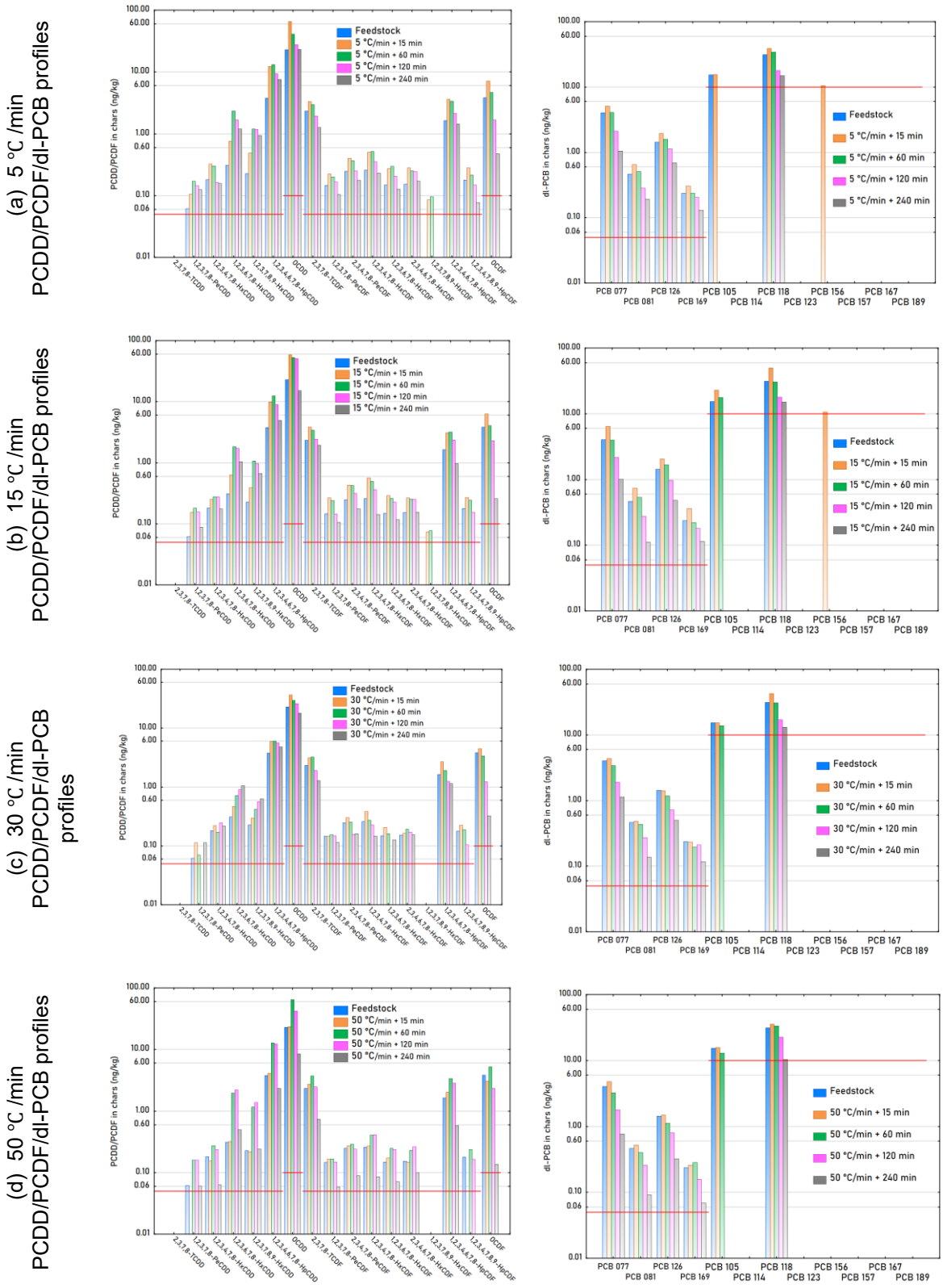

Fig. 2. (a–d) Absolute concentrations of individual PCDD/PCDF and dl-PCB congeners across different HR and RT in torrefied biomass (feedstock: bark, temperature: 260 ºC). Panels plot data using the zero-concentration approach. Measurement uncertainty has not been included on the bars for better readability – it can be found in Tables A1-A5 in the Appendix. The red line in the panels represents LOQ.

Main Findings from PCA and Correlation Analysis

Principal component analysis (PCA; Figs. 3a,b) confirms that the toxicity of torrefied biomass was altered by variations in heating rate (HR) and residence time (RT). In the score plot (Fig. 3a), data points are clustered primarily according to RT, whereas the colored arrows are used to delineate detoxification pathways characteristic of HR. The blue and purple arrows (5 and 15 °C·min^{-1}) overlap, indicating that similar detoxification pathways are followed. In contrast, 30 °C·min^{-1} (orange arrow) was observed to follow a distinct pathway, reflecting limited formation of PCDD/PCDF/dl-PCB from precursors. At HR 50 °C·min^{-1}, a characteristic "delay effect" in precursor formation was observed, after which the detoxification trajectory partially converged with those observed at slower HR. These findings underscore the importance of HR and RT optimization to produce low-dioxin torrefied biomass capable of complying with legislative requirements for environmental applications (noting that this applies only to PCDD/PCDF/dl-PCB thresholds).

Correlation analysis (Fig. 3c) further demonstrated that TEQ values were not consistently correlated across compound groups (*e.g.*, TEQ-PCDD *vs*. TEQ-PCDF). This observation emphasizes the need for individual evaluation of compound groups and elucidation of the underlying mechanistic transformation pathways.

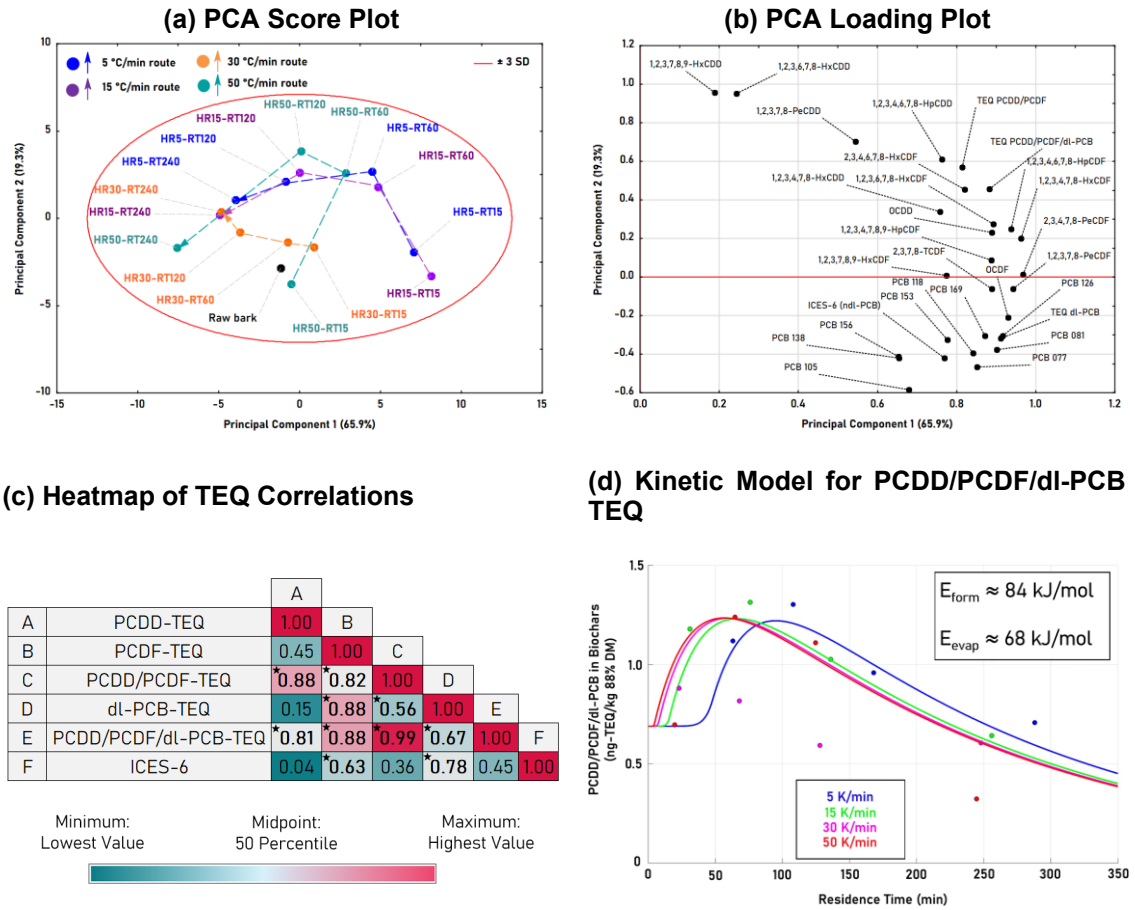

Fig. 3. Results of the statistical analysis. (a–b) Principal Component Analysis (PCA); (c) Correlation analysis; and (d) Kinetic Model for PCDD/PCDF/dl-PCB TEQ evolution. All graphical representations and statistical analyses rely on the LOQ/2 dataset. Correlations marked in bold and with an asterisk are statistically significant.

Technical and Legal Implications for Environmental Applications

Torrefied biomass, although often not formally classified as biochar, encounters both technical and regulatory barriers that limit its environmental application. This subsection examines the recommendations and legal thresholds applicable to biomass-derived chars for environmental uses, including soil and feed additives. Table 3 summarizes the regulations and recommendations established by the World Biochar Certificate (WBC), the European Biochar Certificate (EBC), Commission Delegated Regulation of February 3, 2026, and Directive 2002/32/EC. Noteworthy, the bark evaluated in this experiment was applied exclusively as a model biomass matrix to mechanistically investigate the formation and transformation pathways of PCDD/PCDF/dl-PCB in torrefied biomass, as well as to assess the optimization of HR and RT parameters for preventing potential exceedance of regulatory thresholds and achieving a satisfactory level of detoxification. Accordingly, this material was not selected for its suitability as a fertilizer or carbon sink (or any specified use); therefore, its physicochemical properties should not be interpreted directly in terms of agronomic applicability. Within the scope of this article and discussion, issues related to production temperature, the H/C_{org} ratio, and the PCDD/PCDF/dl-PCB limit are explicitly addressed below, as these parameters are central to the scientific objectives of the study. With respect to regulatory limits and requirements for other compounds and related aspects (allowing a given biomass-derived char to be classified as suitable for a specified application), consultation of the reference documents cited in this subsection is recommended, as they are beyond the scope of this article and discussion.

The first document, namely the newly adopted delegated regulation of the European Commission (European Commision 2026), establishes the parameters governing biochar intended for soil application or incorporation into materials. According to the document, chars for carbon removal activities are recognized as requiring production temperatures of *at least* 350 °C. In addition, carbon removal units are not eligible for issuance for any batch of biochar in which the H/C_{org} ratio is greater than 0.7. The regulation establishes PCDD/PCDF and PCB limits of 20 ng TEQ·kg^{-1} DM and 200 000 ng·kg^{-1} DM, respectively, for applications to agricultural, forest, and other soils, as well as for the incorporation of biochar into materials. The document imposes more stringent limits when biochar is applied to soil indirectly through manure following its use as a livestock feed additive, as presented in Table 3. Under these conditions, compliance with a lower H/C_{org} ratio and the use of a specified feedstock are also required (production is restricted to pure plant biomass or biomass fuel derived exclusively from pure plant biomass).

The subsequent documents presented in Table 3 were developed by the EBC and the WBC, which are voluntary organizations. The WBC is linked to EBC, and both standards were developed by the Ithaka Institute and are owned by Carbon Standards International (EBC 2012-2025a, WBC 2023a). Torrefied biomasses are not classified as biochar by these organizations, which define *biochar* as a product of thermal conversion carried out at temperatures from 350 to 1000 °C (WBC) or above 350 °C (EBC) (EBC 2012-2025a; WBC 2023a). For most certifications, the EBC and WBC establish a PCDD/PCDF limit of 20 ng TEQ·kg^{-1} DM and a PCB limit of 200 000 ng·kg^{-1} DM, apart from the EBC FeedPlus certification, which adopts the limits specified in Directive 2002/32/EC. Similarly, depending on the certification or feedstock type (as specified in the annexes to the EBC and WBC standards), the H/C_{org} ratio must be below 0.7 or 0.4.

Table 3. Recommended or Regulated Limits for PCDD/PCDF and other Parameters, Depending on the Reference and Pathway of Biochar Application

Reference	Application	Temperature*	H/C_{org}	PCDD/PCDF and PCB
Commission Delegated Regulation (EU) 2026/285	Biochar used in agricultural and forest soils	at least 350 °C	no greater than 0.7	20 ng TEQ·kg^{-1} DM for PCDD/PCDF (WHO-TEQ 2005) 200 000 ng·kg^{-1} DM for PCB
	Biochar applied to the soil (agricultural and forest) in the form of manure after being used as a feed additive for livestock	at least 350 °C	no greater than 0.4	0.75 ng TEQ·kg^{-1} 88% DM for PCDD/PCDF (WHO-TEQ 2005) 1.25 ng TEQ·kg^{-1} 88% DM for PCDD/PCDF + dl-PCB (WHO-TEQ 2005) 10 ng·kg^{-1} 88% DM for 6 DIN PCB
	Biochar incorporated into products or applied to soils other than agricultural and forest soils	at least 350 °C	no greater than 0.7	20 ng TEQ·kg^{-1} DM for PCDD/PCDF (WHO-TEQ 2005) 200 000 ng·kg^{-1} DM for PCB
European Biochar Certificate Standard 10.5E	EBC-FeedPlus Certification (feed additive and agricultural soil)	above 500 °C	<0.4	0.5 ng TEQ·kg^{-1} 88% DM for PCDD/PCDF (WHO-TEQ 2005) – trigger value 0.75 ng TEQ·kg^{-1} 88% DM for PCDD/PCDF (WHO-TEQ 2005) – limit value 0.35 ng TEQ·kg^{-1} 88% DM for dl-PCB (WHO-TEQ 2005) – trigger value 1.25 ng TEQ·kg^{-1} 88% DM for PCDD/PCDF +dl-PCB (WHO-TEQ 2005) – limit value 10 000 ng·kg^{-1} 88% DM for 6 DIN PCB – limit value
	EBC-Agro or EBC-AgroOrganic Certification (soil application)	above 350 °C	<0.7 or <0.4 for specified feedstock	20 ng·kg^{-1} (I-TEQ) for PCDD/PCDF 200 000 ng·kg^{-1} DM for PCB
	EBC-Urban Certification (tree planting, park maintenance, sidewalk embellishments, ornamental plants, and rainwater drainage and filtration)	above 350 °C	<0.7 or <0.4 for specified feedstock	20 ng·kg^{-1} (I-TEQ) for PCDD/PCDF 200 000 ng·kg^{-1} DM for PCB
	EBC-Materials Certification (biochar use in products that may come into direct skin contact with consumers or food-grade products)	above 350 °C or 500 °C for specified feedstock	<0.7 or <0.4 for specified feedstock	20 ng·kg^{-1} (I-TEQ) for PCDD/PCDF 200 000 ng·kg^{-1} DM for PCB
	EBC-Basic Certification (incorporation into materials)	above 350 °C or 500 °C for specified feedstock	<0.7 or <0.4 for specified feedstock	20 ng·kg^{-1} (I-TEQ) for PCDD/PCDF 200 000 ng·kg^{-1} DM for PCB
World Biochar Certificate Standard 1.1	WBC-Premium Certification (all applications)	above 350 °C or 500 °C for specified feedstock	<0.4	20 ng·kg^{-1} (I-TEQ) for PCDD/PCDF 200 000 ng·kg^{-1} DM for PCB
	WBC-Agro Certification (soil use)	above 350 °C or 500 °C for specified feedstock	<0.7 or <0.4 for specified feedstock	20 ng·kg^{-1} (I-TEQ) for PCDD/PCDF 200 000 ng·kg^{-1} DM for PCB
	WBC-Materials Certification (incorporation into materials)	above 350 °C or 500 °C for specified feedstock	<0.7 or <0.4 for specified feedstock	20 ng·kg^{-1} (I-TEQ) for PCDD/PCDF 200 000 ng·kg^{-1} DM for PCB
Directive 2002/32/EC	Feed additive	not specified	not specified	0.5 ng TEQ·kg^{-1} 88% DM for PCDD/PCDF (WHO-TEQ 2005) – trigger value 0.75 ng TEQ·kg^{-1} 88% DM for PCDD/PCDF (WHO-TEQ 2005) – limit value 0.35 ng TEQ·kg^{-1} 88% DM for dl-PCB (WHO-TEQ 2005) – trigger value 1.25 ng TEQ·kg^{-1} 88% DM for PCDD/PCDF +dl-PCB (WHO-TEQ 2005) – limit value 10 000 ng·kg^{-1} 88% DM for 6 DIN PCB – limit value

* The temperature threshold of 350°C cited in the WBC and EBC documents derives from their definition of biochar, whereas a minimum temperature of 500°C is prescribed for EBC-FeedPlus certification and is also required for certain problematic feedstocks under other certification schemes.

However, the minimum temperature is not explicitly defined in these documents; therefore, in the table, we have adopted the temperature specified in the respective definitions. An exception applies to the EBC FeedPlus certification, which requires a minimum temperature of 500 °C. In the context of other certifications, this temperature threshold is also mandated for certain problematic feedstocks. Both EBC and WBC prescribe lists of permissible biomass sources for the production of biochar under specific certification schemes (EBC 2012-2025b; WBC 2023b). Recently, Carbon Standards International updated list of permissible matrices for the establishment of biochar C-sinks ($H/C_{org} < 0.4$) has also been published (Carbon Standards International 2025). For other certification guidelines, the authors refer readers to the WBC and EBC standards (EBC 2012-2025a, WBC 2023a).

In the context of feed additives, maximum content values for feed materials of plant origin have been established by the European Union in accordance with Directive 2002/32/EC (European-Union 2002) – the last document presented in the Table 3. The PCDD/PCDF maximum content is restricted to 0.75 ng TEQ·kg^{-1} (88% DM), and the PCDD/PCDF/dl-PCB maximum content is restricted to 1.25 ng TEQ·kg^{-1} (88% DM). Action thresholds have been set at 0.5 ng TEQ·kg^{-1} (88% DM) for PCDD/PCDF and 0.35 ng TEQ·kg^{-1} (88% DM) for dl-PCB. The TEQ of the limits mentioned refers to the WHO 2005 methodology. The maximum content of non-dioxin-like PCB (ICES-6) has been fixed at 10 000 ng·kg^{-1} (88% DM) for feed materials of plant origin (European-Union 2002). Consequently, an inconsistency exists between the Directive and the new European Commission regulation regarding the limit for 6 DIN PCB, and the value specified in the Directive appears to be the correct one. It should be noted that the Directive establishes general limits for feed additives rather than specifically for biochar, which explains the absence of requirements regarding production temperature or the H/C_{org} ratio.

In view of these regulatory requirements, the application of torrefaction as a method for producing chars for environmental use may be regarded as problematic. It is worth noting that the primary scientific objective of the authors was to perform a mechanistic analysis of PCDD/PCDF transformations during torrefaction and detoxification potential under varying HR and RT conditions, considering the environmental implications in the context of their theoretical future application. Although current regulatory frameworks impose significant limitations on the practical use of these materials, the obtained results may provide valuable insights for the future development of low-temperature-derived products. For example, studies by Szufa *et al*. (2025) demonstrated that the addition of torrefied woody biomass (produced in a superheated steam atmosphere) can increase net photosynthetic growth, accelerate growth kinetics, and enhance the final height of the *Lemna minor* L. This demonstrates that a low energy thermo-chemical process such as torrefaction can be more reasonable from economical point of view techniques compared to pyrolysis, which needs higher temperatures for production biochars as a plant growth stimulator. Additionally, Farci *et al*. (2021) showed that torrefaction improves the digestibility of barley as horse feed (foregut digestibility and hindgut fermentation of barley *in vitro*).

The use of similar products derived from other low-temperature processes may also be beneficial. Hydrochar (a product of wet torrefaction, also termed hydrothermal carbonization) derived from aerobically digested sewage sludge was recently produced and characterized by Wilk *et al*. (2026) at 210 °C with a residence time of 2 h. Toxicity tests of aqueous hydrochar extracts were conducted to evaluate their inhibitory effects on crustaceans, bacteria, and macrophytes. In addition, the influence of hydrochar on mono-

and di-cotyledonous plants was assessed through direct application. The results demonstrated that aqueous hydrochar extracts were toxic to crustaceans and bacteria; however, no inhibitory effects were observed for macrophytes. Moreover, a stimulating effect on the above-ground parts of *Hordeum vulgare* and *Sinapis alba* was reported. In contrast, the direct application of hydrochar inhibited the growth of the evaluated plants. The findings, therefore, indicate an interesting possibility for the use of hydrochar aqueous extract to stimulate the growth of above-ground plant parts.

Nevertheless, independent of specific legal classifications, thermal processing temperature is, in the authors' view, more appropriately treated as a flexible operational parameter, conditioned by the detoxification requirements of the raw material and the target physicochemical properties to be achieved, thereby enabling the production of chars in an environmentally and economically sustainable manner. Previous studies have demonstrated that torrefied biomass can attain H/C ratios of < 0.7 (Olugbade and Ojo 2020). Moreover, H/C ratios approaching or even below 0.4 can be achieved (Almutairi *et al*. 2023), which— potentially provided that additional regulatory criteria are satisfied— could permit classification of such materials as feed additives. Furthermore, the present study, together with prior investigations (Sobol *et al*. 2025a), has demonstrated that substantial detoxification of biomass with respect to PCDD/PCDF/dl-PCB can be achieved through the application of appropriate torrefaction parameters, including temperature, heating rate (HR), and residence time (RT).

As mentioned previously, an additional promising application of torrefaction is its deployment as a pre-treatment stage before targeted pyrolysis. In the study by Han *et al*. (2021), torrefaction at 300 °C (60 min) was applied as a pre-treatment step before the pyrolysis of wood (poplar) and polyvinyl chloride, and a reduction of 98.63% in total dioxin content and 99.09% in the toxic equivalent of volatile dioxins was observed relative to direct pyrolysis (however, the concentration of dioxins in the solid phase was found to be 90.65% higher in the scenario involving torrefaction as a pre-treatment followed by pyrolysis, compared to the solid phase obtained after direct pyrolysis). The phenomenon observed by Han *et al.* (2021) can be explained by the phase distribution of the precursors. While torrefaction effectively removes a large portion of chlorine as HCl and stunts dioxin synthesis in the volatile phase, the thermal decomposition leaves a solid residue that contributes to an increase in the amount of polycyclic aromatic hydrocarbons (PAHs). During the subsequent pyrolysis stage, these retained PAHs and the remaining active chlorine in the solid matrix react, which enhances chlorination reactions directly in the solid phase. This leads to a localized increase in fixed dioxins within the solid product (char), even though the overall and volatile dioxin levels are significantly reduced.

Considering these findings, future research should be directed toward the development of two-stage biomass detoxification strategies based on torrefaction (with the parameters that enable the solid phase detoxification) followed by pyrolysis, with the objective of achieving target physicochemical properties of biochar for specified use. Although a lower temperature (260 °C) was applied in the present study, it was demonstrated that the residence time (RT = 60 min) used by Han *et al*. (2021) was insufficient to achieve effective detoxification of the solid phase in torrefaction.

However, it must be emphasized that the stabilization and detoxification of PCDD/PCDF/dl-PCB in torrefied biomass through the application of optimized technological parameters—demonstrated in the present and previous studies (Sobol *et al*. 2025a)—and the potential application of these outcomes into a two-stage process requires further investigation, experimental validation, and systematic re-evaluation of biochar

toxicity following pyrolysis. For the two-stage process, a systematic investigation of dioxins across all phases is strongly recommended, including the feedstock, the products formed after the first stage, and those obtained after the second stage (and their comparison with the products obtained from direct pyrolysis), in order to determine the complete detoxification performance of the system. In addition, the evaluation of the two-stage system under variable pyrolysis temperatures should be considered, as this would enable a more detailed understanding of the underlying mechanistic processes.

CONCLUSIONS

1. Short torrefaction times (RTs) (up to 60 min) were demonstrated to trigger an approximately twofold increase in torrefied biomass toxicity (up to 1.314 ± 0.197 ng-TEQ·kg^{-1}, 88% DM), arising from precursor-mediated formation of PCDD/PCDF/dl-PCB.
2. Extension of the RT was shown to drive torrefied biomass detoxification, with toxicity after 240 min ranging from substantially lower levels (0.324 ± 0.049 ng-TEQ·kg^{-1}, 88% DM) to values comparable (0.707 ± 0.106 ng-TEQ·kg^{-1}, 88% DM) to the raw biomass (0.689 ± 0.103 ng-TEQ·kg^{-1}, 88% DM) in terms of PCDD/PCDF/dl-PCB.
3. The formation pathways of PCDD/PCDF/dl-PCB were strongly modulated by the heating rate (HR), as evidenced by a distinct kinetic profile at 30 °C·min^{-1}, which constrained precursor-driven formation, and by the characteristic "*delay effect*" at HR 50 °C·min^{-1}, where PCDD/PCDF/dl-PCB formation was temporally shifted relative to other heating rates.
4. Future research should investigate the use of torrefied biomass in environmental applications to strengthen its competitiveness and systematically evaluate its advantages and limitations relative to conventional biochar-based applications.
5. There is a growing need to establish regulations or guidelines governing the use of torrefied biomass in non-energy applications, as existing regulatory frameworks and guidance documents focus primarily on biochar, thereby constraining the broader deployment of torrefied biomass.
6. The findings of this study indicate that optimizing HR and RT can mitigate the toxicity of torrefied biomass. Nevertheless, future research should investigate the kinetics of PCDD/PCDF formation from precursor compounds across different temperature regimes and evaluate the potential for reducing the concentrations of these contaminants through appropriate control of the aforementioned process parameters.

ACKNOWLEDGMENTS

ŁS would like to thank the State Forests (Oborniki Śląskie Forest District) for permission to collect bark for research purposes. This work was supported by the Wrocław University of Environmental and Life Sciences (Poland) as part of the research project number N070/0009/24. The authors gratefully acknowledge financial support from the BioTrainValue project (BIOmass Valorisation *via* Superheated Steam Torrefaction, Pyrolysis, Gasification Amplified by Multidisciplinary Researchers TRAINing for

Multiple Energy and Products' VALUEs) and also funded by the Horizon Europe Marie Skłodowska-Curie Staff Exchange programme under project number 101086411. ŁS would like to thank Dr. Jannis Grafmüller for his preliminary review of the chapter "Technical and Legal Implications for Environmental Applications".

Use of Generative AI

The authors used AI-based tools to enhance the readability and linguistic quality of the manuscript. All AI-assisted revisions were carefully reviewed and validated by the authors before submission. The authors assume full responsibility for the content of the publication.

REFERENCES CITED

Addink, R., and Altwicker, E. (2004). "Formation of polychlorinated dibenzo--dioxins and dibenzofurans on secondary combustor/boiler ash from a rotary kiln burning hazardous waste," *Journal of Hazardous Materials*, 114(1–3), 53-57. https://doi.org/10.1016/j.jhazmat.2004.06.031

Almutairi, A. A., Ahmad, M., Rafique, M. I., and Al-Wabel, M. I. (2023). "Variations in composition and stability of biochars derived from different feedstock types at varying pyrolysis temperature," *Journal of the Saudi Society of Agricultural Sciences*, 22(1), 25-34. https://doi.org/10.1016/j.jssas.2022.05.005

Altarawneh, M., Dlugogorski, B. Z., Kennedy, E. M., and Mackie, J. C. (2009). "Mechanisms for formation, chlorination, dechlorination and destruction of polychlorinated dibenzo-*p*-dioxins and dibenzofurans (PCDD/Fs)," *Progress in Energy and Combustion Science*, 35(3), 245-274. https://doi.org/10.1016/j.pecs.2008.12.001

"BBodSchV Bundes-Bodenschutz- und Altlastenverordnung," (1999). Deutsches Bundesamt für Umwelt, Berlin, Germany.

Blum, W., Horak, O., Mentler, A., and Puschenreiter, M. (2009). "Trace elements," *Environmental and Ecological Chemistry*, Encyclopedia of life support systems. UNESCO Paris, 2, 156–164.

Carbon Standards International. (2025). "Positive list of permissible matrices for the establishment of biochar C-sinks (H/Corg < 0.4)," v3_15: latest update 15.11.2025.

Chandrasekharan Nair, S., John, V., Geetha Bai, R., and Kikas, T. (2025). "Torrefaction of lignocellulosic biomass: A pathway to renewable energy, circular economy, and sustainable agriculture," *Sustainability* 17(17), article 7738. https://doi.org/10.3390/su17177738

Chen, W.-H., Lin, B.-J., Lin, Y.-Y., Chu, Y.-S., Ubando, A. T., Show, P. L., Ong, H. C., Chang, J.-S., Ho, S.-H., Culaba, A. B., Pétrissans, A., and Pétrissans, M. (2021). "Progress in biomass torrefaction: Principles, applications and challenges," *Progress in Energy and Combustion Science* 82, article 100887. https://doi.org/10.1016/j.pecs.2020.100887

Cheruiyot, N. K., Lee, W.-J., Yan, P., Mwangi, J. K., Wang, L.-C., Gao, X., Lin, N.-H., and Chang-Chien, G.-P. (2016). "An overview of PCDD/F Inventories and emission factors from stationary and mobile sources: What we know and what is missing," *Aerosol and Air Quality Research*, 16(12), 2965-2988. https://doi.org/10.4209/aaqr.2016.10.0447

Cieplik, M. K., Carbonell, J. P., Muñoz, C., Baker, S., Krüger, S., Liljelind, P., Marklund, S., and Louw, R. (2003). "On dioxin formation in iron ore sintering," *Environmental Science & Technology* 37(15), 3323-3331. https://doi.org/10.1021/es026292g

Conesa, J. A., and Mortes, J. (2025). "The contribution of commercial flights to the global emissions of inorganic and organic pollutants," *Processes* 13(4), article 995. https://doi.org/10.3390/pr13040995

EBC. (2012-2025a). "European Biochar Certificate - Guidelines for a sustainable production of biochar," Carbon Standards International (CSI), Frick, Switzerland. (http://carbon-standards.com/ebc). Version 10.5E from 14th August 2025.

EBC. (2012-2025b). "Positive list of permissible biomasses for the production of biochar," European Biochar Certificate.

European Commision. (2026). "Commission Delegated Regulation (EU) 2026/285 of 3 February 2026 supplementing Regulation (EU) 2024/3012 of the European Parliament and of the Council by establishing the certification methodologies for permanent carbon removals activities."

European-Union. (2002). "Directive 2002/32/EC of the European Parliament and of the Council," Off. J. Eur. Communities.

Farci, V., Murray, J.-A., and Hastie, P. (2021). "52 Evaluation of barley digestibility with an in vitro total tract digestion simulation," *Journal of Equine Veterinary Science*, 100, article 103515. https://doi.org/10.1016/j.jevs.2021.103515

Gao, Q., Cieplik, M. K., Budarin, V. L., Gronnow, M., and Jansson, S. (2016). "Mechanistic evaluation of polychlorinated dibenzo-p-dioxin, dibenzofuran and naphthalene isomer fingerprints in microwave pyrolysis of biomass," *Chemosphere*, 150, 168-175. https://doi.org/10.1016/j.chemosphere.2016.02.031

Gao, Q., Edo, M., Larsson, S. H., Collina, E., Rudolfsson, M., Gallina, M., Oluwoye, I., Altarawneh, M., Dlugogorski, B. Z., and Jansson, S. (2017). "Formation of PCDDs and PCDFs in the torrefaction of biomass with different chemical composition," *Journal of Analytical and Applied Pyrolysis*, 123, 126-133. https://doi.org/10.1016/j.jaap.2016.12.015

García-Bermejo, Á., Herrero, L., González, M.-J., and Gómara, B. (2017). "Occurrence and estimated dietary intake of PCBs and PCDD/Fs in functional foods enriched with omega-3 from Spain," *Journal of Agricultural and Food Chemistry* 65(16), 3396-3405. https://doi.org/10.1021/acs.jafc.7b00785

Gonzales, T. D. S., Monteiro, S., Lamas, G. C., Rodrigues, P. P. O., Siqueira, M. B. B., Follegatti-Romero, L. A., and Silveira, E. A. (2025). "Simulation and thermodynamic evaluation of woody biomass waste torrefaction," *ACS Omega* 10(4), 3585-3597. https://doi.org/10.1021/acsomega.4c08299

Grafmüller, J., Rathnayake, D., Hagemann, N., Bucheli, T. D., and Schmidt, H.-P. (2024). "Biochars from chlorine-rich feedstock are low in polychlorinated dioxins, furans and biphenyls," *Journal of Analytical and Applied Pyrolysis* 183, article 106764. https://doi.org/10.1016/j.jaap.2024.106764

Gülegen, B., Noori, A. A., and Taşdemir, Y. (2025). "Investigation of temporal PCDD/F concentration levels and gas/particle partitioning employing recent models in the ambient air of a wastewater treatment plant site," *Atmospheric Pollution Research*, article 102823. https://doi.org/10.1016/j.apr.2025.102823

Hale, S. E., Lehmann, J., Rutherford, D., Zimmerman, A. R., Bachmann, R. T., Shitumbanuma, V., O'Toole, A., Sundqvist, K. L., Arp, H. P. H., and Cornelissen, G. (2012). "Quantifying the total and bioavailable polycyclic aromatic hydrocarbons and

dioxins in biochars," *Environmental Science & Technology* 46(5), 2830-2838. https://doi.org/10.1021/es203984k

Han, Z., Li, J., Gu, T., Yang, R., Fu, Z., Yan, B., and Chen, G. (2021). "Effects of torrefaction on the formation and distribution of dioxins during wood and PVC pyrolysis: An experimental and mechanistic study," *Journal of Analytical and Applied Pyrolysis* 157, article 105240. https://doi.org/10.1016/j.jaap.2021.105240

IARC. (2012). *Review of Human Carcinogens: Chemical Agents and Related Occupations*, International Agency for Research on Cancer.

Jabeen, S., Gao, X., Hayashi, J., Altarawneh, M., and Dlugogorski, B. Z. (2022). "Systematic characterization of biocrude and aqueous phase from hydrothermal carbonization of algal biomass," *Journal of Environmental Chemical Engineering*, 10(3), article 107953. https://doi.org/10.1016/j.jece.2022.107953

Jindarom, C., Meeyoo, V., Rirksomboon, T., Kitiyanan, B., and Rangsunvigit, P. (2006). "Production of bio-oil by oxidative pyrolysis of sewage sludge in rotating fixed bed reactor," *As. J. Energy Env*. 7(4), 401-409.

Kirkby, E. A. (2012). "Introduction, definition, and classification of nutrients," in: *Marschner's Mineral Nutrition of Plants*, Elsevier, 3-5. https://doi.org/10.1016/B978-0-12-819773-8.00016-2

Lacomba, I., Palomares-Bolaños, J., Juan-García, A., López, A., Olivero-Verbel, J., Caballero-Gallardo, K., Coscollà, C., and Juan, C. (2025). "Levels and risk assessment of dl-PCBs and dioxins in soils surrounded by cement plants from industrial areas of Colombia and Spain," *Emerging Contaminants* 11(1), article 100427. https://doi.org/10.1016/j.emcon.2024.100427

Mason, P. E., Higgins, L., Climent Barba, F., Cunliffe, A., Cheffins, N., Robinson, D., and Jones, J. M. (2020). "An assessment of contaminants in UK road-verge biomass and the implications for use as anaerobic digestion feedstock," *Waste and Biomass Valorization* 11(5), 1971-1981. https://doi.org/10.1007/s12649-018-00557-x

Moscicki, K. J., Niedzwiecki, L., Owczarek, P., and Wnukowski, M. (2014). "Commoditization of biomass: dry torrefaction and pelletization-a review," Journal of power technologies, Warsaw University of Technology, Institute of Heat Engineering, 94(4), 233.

Nair, P. S., P S, S. M., Suresh, S., A J, S., K, S., S, A. K., P R, A., Krishnan, N., S, P., Chakraborty, S., Chopra, H., Akash, S., Amin, R., Dey, A., Alagawany, M., Chandran, D., and Dhama, K. (2023). "Beneficial impacts of biochar as a potential feed additive in animal husbandry," *Journal of Experimental Biology and Agricultural Sciences* 11(3), 479-499. https://doi.org/10.18006/2023.11(3).479.499

Nganai, S., Dellinger, B., and Lomnicki, S. (2014). "PCDD/PCDF ratio in the precursor formation model over CuO surface," *Environmental Science & Technology* 48(23), 13864-13870. https://doi.org/10.1021/es504253w

Olugbade, T. O., and Ojo, O. T. (2020). "Biomass torrefaction for the production of high-grade solid biofuels: A review," *BioEnergy Research* 13(4), 999-1015. https://doi.org/10.1007/s12155-020-10138-3

Piskorska-Pliszczynska, J., Mikolajczyk, S., Warenik-Bany, M., Maszewski, S., and Strucinski, P. (2014). "Soil as a source of dioxin contamination in eggs from free-range hens on a Polish farm," *Science of The Total Environment* 466–467, 447-454. https://doi.org/10.1016/j.scitotenv.2013.07.061

Praud, D., Amadou, A., Coudon, T., Duboeuf, M., Mercoeur, B., Faure, E., Grassot, L., Danjou, A. Mn., Salizzoni, P., Couvidat, F., Dossus, L., Severi, G., Mancini, F. R.,

and Fervers, B. (2025). "Association between chronic long-term exposure to airborne dioxins and breast cancer," *International Journal of Hygiene and Environmental Health* 263, article 114489. https://doi.org/10.1016/j.ijheh.2024.114489

Rao, Q., Wang, X., Zhang, Q., Hoogenboom, R., Li, H., Deng, Z., Song, W., Cheng, L., Liu, X., Guan, S., Song, W., Yao, C., Chen, S., and Zhou, J. (2022). "New insights into the transfer and accumulation of dioxins and dioxin-like PCBs in the food web of farmed Chinese mitten crabs: A typical case from the Yangtze River area," *Journal of Hazardous Materials* 436, article 129178. https://doi.org/10.1016/j.jhazmat.2022.129178

Rodriguez, C., Cook, A., Devine, B., Van Buynder, P., Lugg, R., Linge, K., and Weinstein, P. (2008). "Dioxins, furans and PCBs in recycled water for indirect potable reuse," *International Journal of Environmental Research and Public Health* 5(5), 356-367. https://doi.org/10.3390/ijerph5050356

Růžičková, J., Šafář, M., Slamová, K., Raclavská, H., Kucbel, M., Švédová, B., Juchelková, D., Brťková, H., and Drozdová, J. (2025). "Production of gaseous VOC/SVOC during softwood torrefaction under various technological conditions," *Environmental Technology & Innovation* 38, article 104086. https://doi.org/10.1016/j.eti.2025.104086

Santa-Marina, L., Barroeta, Z., Irizar, A., Jiménez, B., Gonzalez, P., Muñoz-Arnanz, J., García-Baquero, G., Jimeno-Romero, A., Zubero, M. B., Urbieta, N., Ibarluzea, J., and Lertxundi, A. (2026). "Assessment of PCDD/F and dl-PCB levels in air before and after the start-up of an energy recovery plant in northern Spain," *Environmental Pollution* 388, article 127371. https://doi.org/10.1016/j.envpol.2025.127371

Sobol, Ł., Dyjakon, A., and Soukup, K. (2023). "Dioxins and furans in biochars, hydrochars and torreficates produced by thermochemical conversion of biomass: A review," *Environmental Chemistry Letters* 21(4), 2225-2249. https://doi.org/10.1007/s10311-023-01600-7

Sobol, Ł., Dyjakon, A., Korendał, M., Styczyńska, M., Sabat, D., Szumny, A., and Dlugogorski, B. Z. (2024). "Alteration of biomass toxicity in torrefaction – A XDS-CALUX bioassay study," *Chemosphere* 351, article 141258. https://doi.org/10.1016/j.chemosphere.2024.141258

Sobol, Ł., Długogórski, B. Z., Karczewski, M., Murthy, V., Sabat, D., Styczyńska, M., Telega, P., Zawiślak, I., and Dyjakon, A. (2025a). "Toward dioxin-free chars: Comparative toxicity of biomass valorization pathways under CO_2, N_2, and hydrothermal conditions," *Bioresource Technology* 2025, article 133855. https://doi.org/https://doi.org/10.1016/j.biortech.2025.133855

Sobol, Ł., Dyjakon, A., and Dlugogorski, B. Z. (2025b). "Dioxin-like polychlorinated biphenyls (dl-PCB) in hydrochars and biochars: Review of recent evidence, pollution levels, critical gaps, formation mechanisms and regulations," *Journal of Hazardous Materials* 486, article 136615. https://doi.org/10.1016/j.jhazmat.2024.136615

Sobol, Ł., Telega, P., Dyjakon, A., Zawiślak, I., and Długogórski, B. Z. (2025c). "PCDD/F/PCB emissions from energy generation in Central Europe: uptake mechanisms in biomass, fingerprint profiling and source modeling," *Environment International*, 109909. DOI: 10.1016/j.envint.2025.109909

Sommersacher P., Kienzl N., Evic N., and Hochenauer C. (2018). "The influence of torrefaction on the combustion behaviour of selected agricultural and waste-derived solid biomass fuels," *Chemical Engineering Transactions*, AIDIC: Italian Association of Chemical Engineering, IT, 65, 361–366. DOI: 10.3303/CET1865061

Suthar, R. G., Wang, C., Nunes, M. C. N., Chen, J., Sargent, S. A., Bucklin, R. A., and Gao, B. (2018). "Bamboo biochar pyrolyzed at low temperature improves tomato plant growth and fruit quality," *Agriculture* 8(10), article 153. https://doi.org/10.3390/agriculture8100153

Szufa, S., Unyay, H., Piersa, P., Kędzierska-Sar, A., Romanowska-Duda, Z., and Likozar, B. (2025). "Reduction of spruce phytotoxicity by superheated steam torrefaction and its use in stimulating the growth of ecological bio-products: *Lemna minor* L," *Biomass Conversion and Biorefinery* 15(11), 17739-17760. https://doi.org/10.1007/s13399-025-06508-6

Themba, N., Sibali, L. L., and Chokwe, T. B. (2023). "A review on the formation and remediations of polychlorinated dibenzo p-dioxins and dibenzo-furans (PCDD/Fs) during thermal processes with a focus on MSW process," *Air Quality, Atmosphere & Health* 16(10), 2115-2132. https://doi.org/10.1007/s11869-023-01394-1

Tripathi, J., Causer, T., Ciolkosz, D. E., DeVallance, D. B., Białowiec, A., and Nunes, L. J. R. (2024). "Non-energetic application of carbon-rich torrefied biomass in the bioeconomy: A review," *Biofuels* 15(4), 389-405. https://doi.org/10.1080/17597269.2023.2250974

Tumuluru, J. S., Ghiasi, B., Soelberg, N. R., and Sokhansanj, S. (2021). "Biomass torrefaction process, product properties, reactor types, and moving bed reactor design concepts," *Frontiers in Energy Research* 9, article 728140. https://doi.org/10.3389/fenrg.2021.728140

UNEP (United Nations Environment Programme). (2001). "Stockholm Convention on Persistent Organic Pollutant," UNEP, Genebra.

Urbaniak, M., and Zalewski, M. (2011). "Polychlorinated dibenzo-p-dioxins and polychlorinated dibenzofurans in sediments from two Ethiopian rift valley lakes," *Polish Journal of Environmental Studies* 2011, 20(4).

Wang, X., Rao, Q., Zhang, Q., Liu, C., Li, Y., Wang, D., Huang, D., Li, Y., Yao, C., and Song, W. (2024). "Tissue distribution and exposure risk assessment of dioxins, dioxin-like polychlorinated biphenyls and perfluoroalkyl substances in red swamp crayfish," *Food Control* 166, article 110747. https://doi.org/10.1016/j.foodcont.2024.110747

Wang, Z., Lim, C. J., Grace, J. R., Li, H., and Parise, M. R. (2017). "Effects of temperature and particle size on biomass torrefaction in a slot-rectangular spouted bed reactor," *Bioresource Technology*, 244, 281–288. DOI: 10.1016/j.biortech.2017.07.097

WBC. (2023a). "World Biochar Certificate – Guidelines for a Sustainable Production of Biochar and its Certification," Carbon Standards International, Frick, Switzerland, (http://www.european-biochar.org), version 1.1 from 20th December 2024.

WBC. (2023b). "Positive list of permissible biomasses for the production of biochar. Version 1.11," 36_702EN.

Weber, R., Nagai, K., Nishino, J., Shiraishi, H., Ishida, M., Takasuga, T., Konndo, K., and Hiraoka, M. (2002a). "Effects of selected metal oxides on the dechlorination and destruction of PCDD and PCDF," *Chemosphere*, 46(9–10), 1247-1253. https://doi.org/10.1016/S0045-6535(01)00269-7

Weber, R., Takasuga, T., Nagai, K., Shiraishi, H., Sakurai, T., Matuda, T., and Hiraoka, M. (2002b). "Dechlorination and destruction of PCDD, PCDF and PCB on selected fly ash from municipal waste incineration," *Chemosphere*, 46(9–10), 1255-1262. https://doi.org/10.1016/S0045-6535(01)00268-5

WHO (World Health Organization. (2023). "Dioxins," WHO.

Wilk, M., Szkadłubowicz, K., Śliz, M., Magdziarz, A., and Mikusińska, J. (2026). "Biofuel and toxicity characteristics of hydrochar derived from sewage sludge," *Environmental Science and Pollution Research*. https://doi.org/10.1007/s11356-026-37549-7

Yang, M., Luo, B., Shao, J., Zeng, K., Zhang, X., Yang, H., and Chen, H. (2018). "The influence of CO_2 on biomass fast pyrolysis at medium temperatures," *Journal of Renewable and Sustainable Energy* 10(1), article 013108. https://doi.org/10.1063/1.5005013

Zhang, M., and Buekens, A. (2016). "De novo synthesis of dioxins: A review," *International Journal of Environment and Pollution* 60(1/2/3/4), 63. https://doi.org/10.1504/IJEP.2016.082115

Zhang, C., Wang, M., Chen, W.-H. H., Zhang, Y., Pétrissans, A., Pétrissans, M., and Ho, S.-H. H. (2023a). "Superhydrophobic and superlipophilic biochar produced from microalga torrefaction and modification for upgrading fuel properties," *Biochar* 5(1), 18. https://doi.org/10.1007/s42773-023-00217-x

Zhang, M., Fujimori, T., Lin, X., and Li, X. (2023b). "Formation of PCDD/F catalysed by chromium chloride: experiments and PCDD/F signatures," *Journal of Material Cycles and Waste Management* 25(6), 3801-3811. https://doi.org/10.1007/s10163-023-01798-2

Zhang, S., Zhang, Y., Zhang, X., Xing, D., Hu, J., Zhao, Z., and Yao, L. (2025). "Physicochemical properties of torrefied biomass at different atmosphere: A review," *Industrial Crops and Products* 236, article 121988. https://doi.org/10.1016/j.indcrop.2025.121988

Article submitted: March 9, 2026; Peer review completed: May 25, 2026; Revised version received and accepted: June 8, 2026; Published: June 17, 2026.
DOI: 10.15376/biores.21.3.7074-7108

APPENDIX

TEXT A1. Mathematical Formulation of the Kinetic Model

1. Kinetic Scheme and General Assumptions

The proposed kinetic model treats the torrefied biomass particle as a homogeneous, non-isothermal batch reactor. The model is based on three competing pseudo-first-order reactions:

- Pathway 1 (Formation): Catalytic conversion of solid-phase precursors (P) into PCDD/PCDF/dl-PCB (D). Kinetic constant: k_1.
- Pathway 2 (Evaporation): Physical loss/volatilization of precursors into the gas phase (V). Kinetic constant: k_2.
- Pathway 3 (Detoxification): Dechlorination/degradation of dioxins into non-toxic products (U). Kinetic constant: k_3.

The following physicochemical constraints were imposed during modeling:

- Activation energies (E_i) must be physically meaningful for thermal processes (E_i> 60 kJ·mol^{-1}).
- The activation energy for physical evaporation is lower than that of the chemical formation pathway ($E_2 < E_1$).

2. System of Ordinary Differential Equations (ODEs)

Let C_P and C_D represent the concentration (or toxicity equivalent, TEQ) of precursors and dioxins in the solid phase, respectively. The dynamic evolution of the system is described by the following mass balances:

$$\frac{dC_P}{dt} = -(k_1 + k_2)C_P \quad (1)$$

$$\frac{dC_D}{dt} = k_1 C_P - k_3 C_D \quad (2)$$

Where: C_P is the concentration of precursors (ng·kg^{-1} or ng-TEQ·kg^{-1} 88% DM), C_D is the concentration of dioxins (ng·kg^{-1} or ng-TEQ·kg^{-1} 88% DM), and k is the kinetic constant (s^{-1}).

The kinetic rate constants (k_i) follow the Arrhenius equation:

$$k_i = A_i \exp\left(\frac{-E_i}{R \cdot T(t)}\right) \quad for\ i = 1,2,3 \quad (3)$$

Where A_i is the pre-exponential factor (s^{-1}), E_i is the activation energy (J·mol^{-1}), R is the universal gas constant (J·mol^{-1}·K^{-1}), and T(t) is the absolute temperature (K).

3. Non-isothermal Temperature Profile

The dynamic temperature profile inside the reactor is dictated by the specific heating rate (β) up to the constant torrefaction temperature (T_{max} = 533.15 K):

$$T(t) = \min\left(T_0 + \beta t, T_{max}\right) \quad (4)$$

4. Numerical Discretization and Parameter Estimation

The ODE system was solved numerically using the finite-difference method. Applying a temporal discretization step (Δt), the explicit scheme updates the concentrations iteratively at each time step 'n':

$$C_P^{n+1} = C_P^n - \Delta t\,(k_1^n + k_2^n)C_P^n \quad (5)$$

$$C_D^{n+1} = C_D^n - \Delta t\,(k_1^n C_P^n + k_3^n C_D^n) \quad (6)$$

To estimate the kinetic parameters, we defined an Objective Function (OF) based on the sum of squared residuals between the experimental TEQ values ($C_{D,exp}$) and the model predictions ($C_{D,calc}$) across all N data points:

$$OF = \sum_{j=1}^{N} (C_{D,exp,j} - C_{D,calc,j})^2 \quad (7)$$

The minimization of the OF was performed using the Nelder-Mead simplex nonlinear optimization algorithm. The initial precursor concentration at t=0 ($C_{P,0}$) was also treated as a bounded fitting parameter.

Table A1. Concentrations of PCDD/PCDF/dl-PCB and ndl-PCB Detected in Raw Biomass

Group	Congener	C	U
PCDD (ng/kg)	2,3,7,8-TCDD	0.050	0.010
	1,2,3,7,8-PeCDD	0.062	0.012
	1,2,3,4,7,8-HxCDD	0.181	0.036
	1,2,3,6,7,8-HxCDD	0.309	0.062
	1,2,3,7,8,9-HxCDD	0.229	0.046
	1,2,3,4,6,7,8-HpCDD	3.781	0.756
	OCDD	22.939	4.588
PCDF (ng/kg)	2,3,7,8-TCDF	2.327	0.465
	1,2,3,7,8-PeCDF	0.146	0.029
	2,3,4,7,8-PeCDF	0.249	0.050
	1,2,3,4,7,8-HxCDF	0.258	0.052
	1,2,3,6,7,8-HxCDF	0.149	0.030
	2,3,4,6,7,8-HxCDF	0.152	0.030
	1,2,3,7,8,9-HxCDF	0.050	0.010
	1,2,3,4,6,7,8-HpCDF	1.629	0.326
	1,2,3,4,7,8,9-HpCDF	0.178	0.036
	OCDF	3.831	0.766
dl-PCB (ng/kg)	PCB 077	4.039	0.808
	PCB 081	0.463	0.093
	PCB 126	1.431	0.286
	PCB 169	0.235	0.047
	PCB 105	15.324	3.065
	PCB 114	10	2
	PCB 118	31.135	6.227
	PCB 123	10	2
	PCB 156	10	2
	PCB 157	10	2
	PCB 167	10	2
	PCB 189	10	2
ndl-PCB (ug/kg)	PCB 028	0.100	0.020
	PCB 052	0.100	0.020
	PCB 101	0.100	0.020
	PCB 138	0.100	0.020
	PCB 153	0.100	0.020
	PCB 180	0.100	0.020

*Congeners with concentrations below the LOQ are marked in red, for these entries. The concentration was assumed to equal the LOQ.

Table A2. Concentrations of PCDD/PCDF/dl-PCB and ndl-PCB Detected in Torrefied Biomass Produced with HR 5 °C/min and Different Residence Times

Group	Congener	HR5 – RT15		HR5 – RT60		HR5 – RT120		HR5 – RT240	
		C	U	C	U	C	U	C	U
PCDD (ng/kg)	2,3,7,8-TCDD	0.050	0.010	0.050	0.010	0.050	0.010	0.050	0.010
	1,2,3,7,8-PeCDD	0.105	0.021	0.171	0.034	0.145	0.029	0.125	0.025
	1,2,3,4,7,8-HxCDD	0.322	0.064	0.303	0.061	0.164	0.033	0.157	0.031
	1,2,3,6,7,8-HxCDD	0.759	0.152	2.319	0.464	1.675	0.335	1.195	0.239
	1,2,3,7,8,9-HxCDD	0.490	0.098	1.197	0.239	1.182	0.236	0.940	0.188
	1,2,3,4,6,7,8-HpCDD	12.307	2.461	13.131	2.626	9.334	1.867	7.625	1.525
	OCDD	65.648	13.13	40.778	8.156	27.569	5.514	23.26	4.652
PCDF (ng/kg)	2,3,7,8-TCDF	3.333	0.667	2.947	0.589	1.947	0.389	1.264	0.253
	1,2,3,7,8-PeCDF	0.223	0.045	0.200	0.040	0.167	0.033	0.104	0.021
	2,3,4,7,8-PeCDF	0.402	0.080	0.369	0.074	0.250	0.050	0.177	0.035
	1,2,3,4,7,8-HxCDF	0.506	0.101	0.521	0.104	0.351	0.070	0.232	0.046
	1,2,3,6,7,8-HxCDF	0.273	0.055	0.297	0.059	0.206	0.041	0.128	0.026
	2,3,4,6,7,8-HxCDF	0.283	0.057	0.252	0.050	0.245	0.049	0.171	0.034
	1,2,3,7,8,9-HxCDF	0.086	0.017	0.096	0.019	0.050	0.010	0.050	0.010
	1,2,3,4,6,7,8-HpCDF	3.615	0.723	3.355	0.671	2.140	0.428	1.429	0.286
	1,2,3,4,7,8,9-HpCDF	0.281	0.056	0.215	0.043	0.148	0.030	0.077	0.015
	OCDF	7.157	1.431	4.645	0.929	1.682	0.336	0.477	0.095
dl-PCB (ng/kg)	PCB 077	5.078	1.016	4.085	0.817	2.118	0.424	1.054	0.211
	PCB 081	0.647	0.129	0.510	0.102	0.285	0.057	0.191	0.038
	PCB 126	1.959	0.392	1.594	0.319	1.136	0.227	0.692	0.138
	PCB 169	0.305	0.061	0.236	0.047	0.204	0.041	0.131	0.026
	PCB 105	15.554	3.111	10	2	10	2	10	2
	PCB 114	10	2	10	2	10	2	10	2
	PCB 118	39	7.8	34.359	6.872	17.923	3.585	14.900	2.980
	PCB 123	10	2	10	2	10	2	10	2
	PCB 156	10.560	2.112	10	2	10	2	10	2
	PCB 157	10	2	10	2	10	2	10	2
	PCB 167	10	2	10	2	10	2	10	2
	PCB 189	10	2	10	2	10	2	10	2
ndl-PCB (ug/kg)	PCB 028	0.100	0.020	0.100	0.020	0.100	0.020	0.100	0.020
	PCB 052	0.100	0.020	0.100	0.020	0.100	0.020	0.100	0.020
	PCB 101	0.100	0.020	0.100	0.020	0.100	0.020	0.100	0.020
	PCB 138	0.111	0.022	0.100	0.020	0.100	0.020	0.100	0.020
	PCB 153	0.122	0.024	0.106	0.021	0.100	0.020	0.100	0.020
	PCB 180	0.100	0.020	0.100	0.020	0.100	0.020	0.100	0.020

*Congeners with concentrations below the LOQ are marked in red, for these entries. The concentration was assumed to equal the LOQ.

Table A3. Concentrations of PCDD/PCDF/dl-PCB and ndl-PCB Detected in Torrefied Biomass Produced with HR 15 °C/min and Different Residence Times

Group	Congener	HR15 – RT15		HR15 – RT60		HR15 – RT120		HR15 – RT240	
		C	U	C	U	C	U	C	U
PCDD (ng/kg)	2,3,7,8-TCDD	0.050	0.010	0.050	0.010	0.050	0.010	0.050	0.010
	1,2,3,7,8-PeCDD	0.155	0.031	0.181	0.036	0.157	0.031	0.088	0.018
	1,2,3,4,7,8-HxCDD	0.250	0.050	0.277	0.055	0.276	0.055	0.176	0.035
	1,2,3,6,7,8-HxCDD	0.631	0.126	1.840	0.368	1.738	0.348	1.039	0.208
	1,2,3,7,8,9-HxCDD	0.392	0.078	1.073	0.215	0.962	0.192	0.672	0.134
	1,2,3,4,6,7,8-HpCDD	9.869	1.974	12.392	2.478	9.010	1.802	4.971	0.994
	OCDD	58.043	11.609	52.898	10.58	50.723	10.145	15.131	3.026
PCDF (ng/kg)	2,3,7,8-TCDF	3.820	0.764	3.429	0.686	2.448	0.490	1.944	0.389
	1,2,3,7,8-PeCDF	0.264	0.053	0.241	0.048	0.145	0.029	0.105	0.021
	2,3,4,7,8-PeCDF	0.429	0.086	0.426	0.085	0.316	0.063	0.176	0.035
	1,2,3,4,7,8-HxCDF	0.560	0.112	0.493	0.099	0.365	0.073	0.143	0.029
	1,2,3,6,7,8-HxCDF	0.289	0.058	0.263	0.053	0.228	0.046	0.117	0.023
	2,3,4,6,7,8-HxCDF	0.266	0.053	0.253	0.051	0.250	0.050	0.155	0.031
	1,2,3,7,8,9-HxCDF	0.074	0.015	0.077	0.015	0.050	0.010	0.050	0.010
	1,2,3,4,6,7,8-HpCDF	3.106	0.621	3.190	0.638	2.355	0.471	0.965	0.193
	1,2,3,4,7,8,9-HpCDF	0.271	0.054	0.245	0.049	0.156	0.031	0.050	0.010
	OCDF	6.318	1.264	4.072	0.814	2.314	0.463	0.258	0.052
dl-PCB (ng/kg)	PCB 077	6.445	1.289	4.002	0.800	2.174	0.435	1.008	0.202
	PCB 081	0.735	0.147	0.531	0.106	0.277	0.055	0.112	0.022
	PCB 126	2.046	0.409	1.662	0.332	0.974	0.195	0.481	0.096
	PCB 169	0.361	0.072	0.221	0.044	0.181	0.036	0.114	0.023
	PCB 105	22.961	4.592	17.664	3.533	10	2	10	2
	PCB 114	10	2	10	2	10	2	10	2
	PCB 118	49.625	9.925	30.477	6.095	17.954	3.591	15.086	3.017
	PCB 123	10	2	10	2	10	2	10	2
	PCB 156	10.641	2.128	10	2	10	2	10	2
	PCB 157	10	2	10	2	10	2	10	2
	PCB 167	10	2	10	2	10	2	10	2
	PCB 189	10	2	10	2	10	2	10	2
ndl-PCB (ug/kg)	PCB 028	0.100	0.020	0.100	0.020	0.100	0.020	0.100	0.020
	PCB 052	0.100	0.020	0.100	0.020	0.100	0.020	0.100	0.020
	PCB 101	0.100	0.020	0.100	0.020	0.100	0.020	0.100	0.020
	PCB 138	0.123	0.025	0.100	0.020	0.100	0.020	0.100	0.020
	PCB 153	0.138	0.028	0.101	0.020	0.100	0.020	0.100	0.020
	PCB 180	0.100	0.020	0.100	0.020	0.100	0.020	0.100	0.020

*Congeners with concentrations below the LOQ are marked in red, for these entries. The concentration was assumed to equal the LOQ.

Table A4. Concentrations of PCDD/PCDF/dl-PCB and ndl-PCB Detected in Torrefied Biomass Produced with HR 30 °C/min and Different Residence Times

Group	Congener	HR30 – RT15		HR30 – RT60		HR30 – RT120		HR30 – RT240	
		C	U	C	U	C	U	C	U
PCDD (ng/kg)	2,3,7,8-TCDD	0.050	0.010	0.050	0.010	0.050	0.010	0.050	0.010
	1,2,3,7,8-PeCDD	0.113	0.023	0.070	0.014	0.050	0.010	0.113	0.023
	1,2,3,4,7,8-HxCDD	0.221	0.044	0.172	0.034	0.247	0.049	0.217	0.043
	1,2,3,6,7,8-HxCDD	0.467	0.093	0.718	0.144	0.906	0.181	1.051	0.210
	1,2,3,7,8,9-HxCDD	0.297	0.059	0.421	0.084	0.563	0.113	0.629	0.126
	1,2,3,4,6,7,8-HpCDD	5.907	1.181	6.020	1.204	5.592	1.118	4.832	0.966
	OCDD	36.378	7.276	29.724	5.945	25.862	5.172	17.936	3.587
PCDF (ng/kg)	2,3,7,8-TCDF	3.125	0.625	3.227	0.645	1.905	0.381	1.281	0.256
	1,2,3,7,8-PeCDF	0.146	0.029	0.154	0.031	0.149	0.030	0.115	0.023
	2,3,4,7,8-PeCDF	0.302	0.06	0.256	0.051	0.157	0.031	0.161	0.032
	1,2,3,4,7,8-HxCDF	0.382	0.076	0.272	0.054	0.228	0.046	0.146	0.029
	1,2,3,6,7,8-HxCDF	0.206	0.041	0.161	0.032	0.050	0.010	0.127	0.025
	2,3,4,6,7,8-HxCDF	0.163	0.033	0.192	0.038	0.171	0.034	0.156	0.031
	1,2,3,7,8,9-HxCDF	0.050	0.010	0.050	0.010	0.050	0.010	0.050	0.010
	1,2,3,4,6,7,8-HpCDF	2.694	0.539	1.902	0.380	1.256	0.251	1.154	0.231
	1,2,3,4,7,8,9-HpCDF	0.224	0.045	0.190	0.038	0.104	0.021	0.050	0.010
	OCDF	4.480	0.896	3.353	0.671	1.238	0.248	0.324	0.065
dl-PCB (ng/kg)	PCB 077	4.382	0.876	3.412	0.682	1.897	0.379	1.133	0.227
	PCB 081	0.484	0.097	0.437	0.087	0.272	0.054	0.138	0.028
	PCB 126	1.406	0.281	1.173	0.235	0.720	0.144	0.500	0.100
	PCB 169	0.234	0.047	0.195	0.039	0.210	0.042	0.117	0.023
	PCB 105	15.214	3.043	13.767	2.753	10	2	10	2
	PCB 114	10	2	10	2	10	2	10	2
	PCB 118	42.653	8.531	30.905	6.181	17.075	3.415	13.081	2.616
	PCB 123	10	2	10	2	10	2	10	2
	PCB 156	10	2	10	2	10	2	10	2
	PCB 157	10	2	10	2	10	2	10	2
	PCB 167	10	2	10	2	10	2	10	2
	PCB 189	10	2	10	2	10	2	10	2
ndl-PCB (ug/kg)	PCB 028	0.100	0.020	0.100	0.020	0.100	0.020	0.100	0.020
	PCB 052	0.100	0.020	0.100	0.020	0.100	0.020	0.100	0.020
	PCB 101	0.100	0.020	0.100	0.020	0.100	0.020	0.100	0.020
	PCB 138	0.100	0.020	0.100	0.020	0.100	0.020	0.100	0.020
	PCB 153	0.100	0.020	0.100	0.020	0.100	0.020	0.100	0.020
	PCB 180	0.100	0.020	0.100	0.020	0.100	0.020	0.100	0.020

*Congeners with concentrations below the LOQ are marked in red, for these entries. The concentration was assumed to equal the LOQ.

Table A5. Concentrations of PCDD/PCDF/dl-PCB and ndl-PCB Detected in Torrefied Biomass Produced with HR 50 °C/min and Different Residence Times

Group	Congener	HR50 – RT15		HR50 – RT60		HR50 – RT120		HR50 – RT240	
		C	U	C	U	C	U	C	U
PCDD (ng/kg)	2,3,7,8-TCDD	0.050	0.010	0.050	0.010	0.050	0.010	0.050	0.010
	1,2,3,7,8-PeCDD	0.050	0.010	0.159	0.032	0.159	0.032	0.061	0.012
	1,2,3,4,7,8-HxCDD	0.156	0.031	0.275	0.055	0.236	0.047	0.063	0.013
	1,2,3,6,7,8-HxCDD	0.319	0.064	1.980	0.396	2.216	0.443	0.495	0.099
	1,2,3,7,8,9-HxCDD	0.217	0.043	1.156	0.231	1.377	0.275	0.242	0.048
	1,2,3,4,6,7,8-HpCDD	4.126	0.825	12.737	2.547	12.191	2.438	2.327	0.465
	OCDD	23.598	4.720	64.435	12.887	42.064	8.413	8.533	1.707
PCDF (ng/kg)	2,3,7,8-TCDF	2.726	0.545	3.734	0.747	2.464	0.493	0.736	0.147
	1,2,3,7,8-PeCDF	0.167	0.033	0.166	0.033	0.149	0.030	0.058	0.012
	2,3,4,7,8-PeCDF	0.273	0.055	0.290	0.058	0.241	0.048	0.089	0.018
	1,2,3,4,7,8-HxCDF	0.271	0.054	0.406	0.081	0.415	0.083	0.086	0.017
	1,2,3,6,7,8-HxCDF	0.174	0.035	0.247	0.049	0.236	0.047	0.071	0.014
	2,3,4,6,7,8-HxCDF	0.148	0.030	0.230	0.046	0.261	0.052	0.100	0.020
	1,2,3,7,8,9-HxCDF	0.050	0.010	0.050	0.010	0.050	0.010	0.050	0.010
	1,2,3,4,6,7,8-HpCDF	2.022	0.404	3.370	0.674	2.846	0.569	0.582	0.116
	1,2,3,4,7,8,9-HpCDF	0.050	0.010	0.238	0.048	0.163	0.033	0.050	0.010
	OCDF	3.051	0.610	5.264	1.053	2.343	0.469	0.137	0.027
dl-PCB (ng/kg)	PCB 077	4.768	0.954	3.234	0.647	1.790	0.358	0.768	0.154
	PCB 081	0.518	0.104	0.404	0.081	0.260	0.052	0.092	0.018
	PCB 126	1.479	0.296	1.112	0.222	0.794	0.159	0.322	0.064
	PCB 169	0.259	0.052	0.285	0.057	0.157	0.031	0.069	0.014
	PCB 105	15.664	3.133	12.895	2.579	10	2	10	2
	PCB 114	10	2	10	2	10	2	10	2
	PCB 118	35.382	7.076	33.423	6.685	22.567	4.513	10.389	2.078
	PCB 123	10	2	10	2	10	2	10	2
	PCB 156	10	2	10	2	10	2	10	2
	PCB 157	10	2	10	2	10	2	10	2
	PCB 167	10	2	10	2	10	2	10	2
	PCB 189	10	2	10	2	10	2	10	2
ndl-PCB (ug/kg)	PCB 028	0.100	0.020	0.100	0.020	0.100	0.020	0.100	0.020
	PCB 052	0.100	0.020	0.100	0.020	0.100	0.020	0.100	0.020
	PCB 101	0.100	0.020	0.100	0.020	0.100	0.020	0.100	0.020
	PCB 138	0.100	0.020	0.100	0.020	0.100	0.020	0.100	0.020
	PCB 153	0.104	0.021	0.100	0.020	0.100	0.020	0.100	0.020
	PCB 180	0.100	0.020	0.100	0.020	0.100	0.020	0.100	0.020

*Congeners with concentrations below the LOQ are marked in red, for these entries. The concentration was assumed to equal the LOQ.

Table A6. Concentrations of Chlorinated Phenols and Benzenes in the Feedstock and Selected Torrefied Biomass

Compound	Unit	Raw biomass		HR5 – RT15		HR15 – RT15		HR50 – RT60	
		C	U	C	U	C	U	C	U
2,3,4,5-Tetrachlorophenol	mg/kg DM	<0.010	± 0.003	<0.010	± 0.003	not measured		<0.010	± 0.003
2,3,4,6-Tetrachlorophenol	mg/kg DM	<0.010	± 0.003	<0.010	± 0.003	not measured		<0.010	± 0.003
2,3,4-Trichlorophenol	mg/kg DM	<0.010	± 0.003	<0.010	± 0.003	not measured		<0.010	± 0.003
2,3,5,6-Tetrachlorophenol	mg/kg DM	<0.010	± 0.003	<0.010	± 0.003	not measured		<0.010	± 0.003
2,3,5-Trichlorophenol	mg/kg DM	<0.010	± 0.003	<0.010	± 0.003	not measured		<0.010	± 0.003
2,3,6-Trichlorophenol	mg/kg DM	<0.010	± 0.003	<0.010	± 0.003	not measured		<0.010	± 0.003
2,4,5-Trichlorophenol	mg/kg DM	<0.010	± 0.003	<0.010	± 0.003	not measured		<0.010	± 0.003
2,4,6-Trichlorophenol	mg/kg DM	<0.010	± 0.003	<0.010	± 0.003	not measured		<0.010	± 0.003
2,4-Dichlorophenol	mg/kg DM	<0.010	± 0.003	<0.010	± 0.003	not measured		<0.010	± 0.003
2,6-Dichlorophenol	mg/kg DM	<0.010	± 0.003	<0.010	± 0.003	not measured		<0.010	± 0.003
2-Chlorophenol	mg/kg DM	<0.010	± 0.003	<0.010	± 0.003	not measured		<0.010	± 0.003
3,4,5-Trichlorophenol	mg/kg DM	<0.010	± 0.003	<0.010	± 0.003	not measured		<0.010	± 0.003
Chlorophenols - sum	mg/kg DM	<0.010	± 0.010	<0.010	± 0.010	not measured		<0.010	± 0.010
Pentachlorophenol (PCP)	mg/kg DM	<0.010	± 0.003	<0.010	± 0.003	not measured		<0.010	± 0.003
Dry Matter	%	94.4	± 4.7	98.5	± 4.9	97.8	± 4.9	98.7	± 4.9
1,2,3-Trichlorobenzene	mg/kg DM	<0.005	± 0.0018	<0.005	± 0.0018	<0.005	± 0.0018	<0.005	± 0.0018
1,2,4-Trichlorobenzene	mg/kg DM	<0.005	± 0.0018	<0.005	± 0.0018	<0.005	± 0.0018	<0.005	± 0.0018
1,2-Dichlorobenzene	mg/kg DM	<0.005	± 0.0018	<0.005	± 0.0018	<0.005	± 0.0018	<0.005	± 0.0018
1,3,5-Trichlorobenzene	mg/kg DM	<0.005	± 0.0018	<0.005	± 0.0018	<0.005	± 0.0018	<0.005	± 0.0018
1,3-Dichlorobenzene	mg/kg DM	<0.005	± 0.0018	<0.005	± 0.0018	<0.005	± 0.0018	<0.005	± 0.0018
1,4-dichlorobenzene	mg/kg DM	0.0092	± 0.0032	<0.005	± 0.0018	<0.005	± 0.0018	0.0070	± 0.0025
Chlorobenzene	mg/kg DM	<0.005	± 0.0018	<0.005	± 0.0018	<0.005	± 0.0018	<0.005	± 0.0018

The tests were commissioned to Barg Dolny Śląsk Sp. z o.o (Wrocław, Poland) but performed by its subcontractor (Eurofins OBiKŚ Polska Sp. z o.o, Katowice, Poland). Chlorophenols were determined according to PN-ISO 14154:2008; EFO/I/45/2:17.09.2025, GC-MS/MS. Dry mass was determined by weight method according to PN-ISO 11465:1999 (R). Chlorobenzenes were determined according to PN EN ISO 22155:2016-07 (R), HS-GC-MS. The results are given in the form C ± U, where C is the concentration and U is the expanded measurement uncertainty (calculated for a coefficient k=2, which corresponds to a confidence interval of approx. 95%).

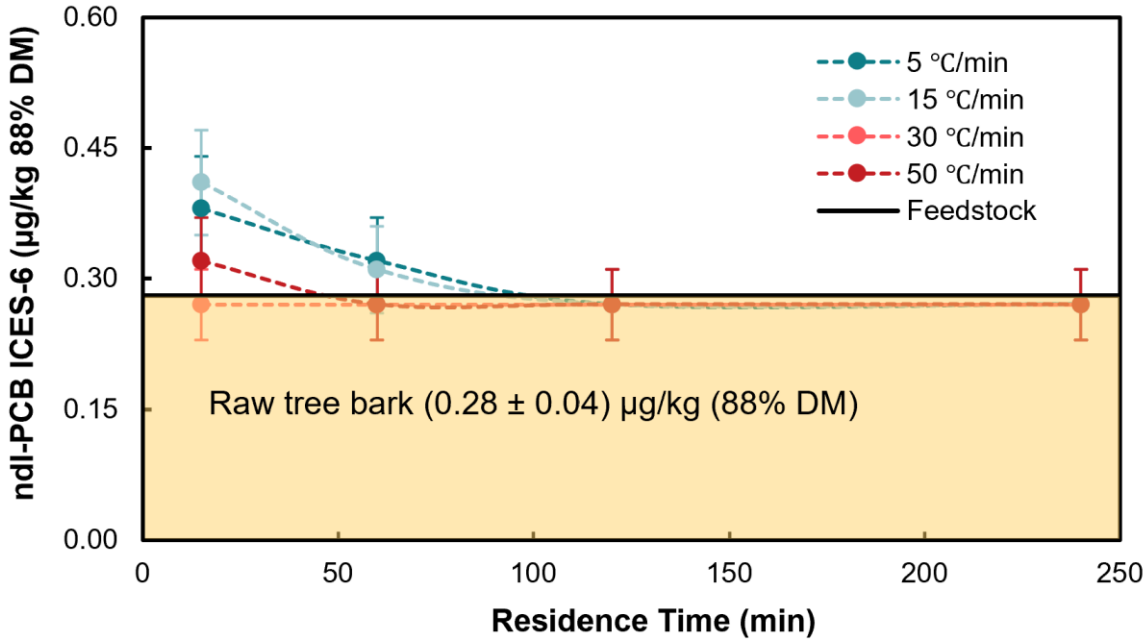

Fig. A1. ICES-6 values of torrefied biomass depending on HR and RT

Fig. A2. Photographs of unprocessed biomass (photographs were taken in a crucible with a diameter of 40 mm)

HR5RT15	HR5RT60	HR5RT120	HR5RT240
		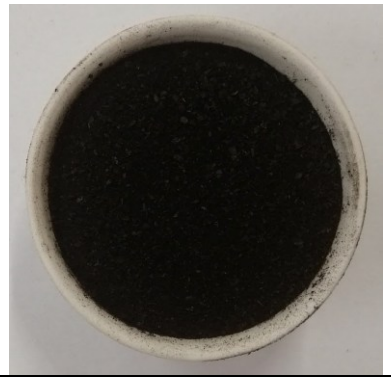	
HR15RT15	**HR15RT60**	**HR15RT120**	**HR15RT240**
		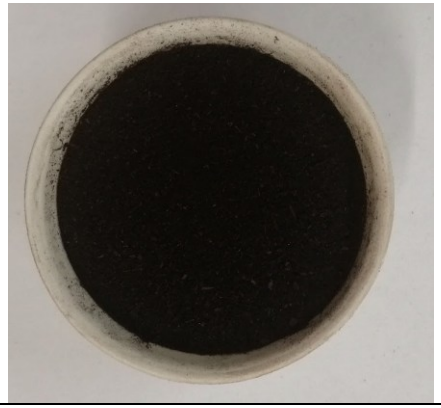	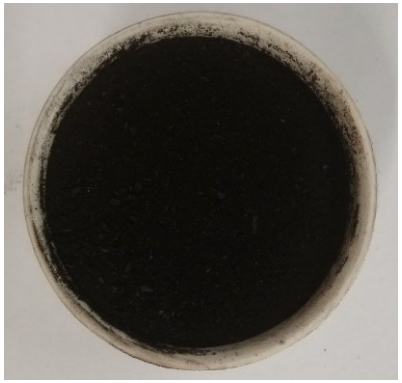

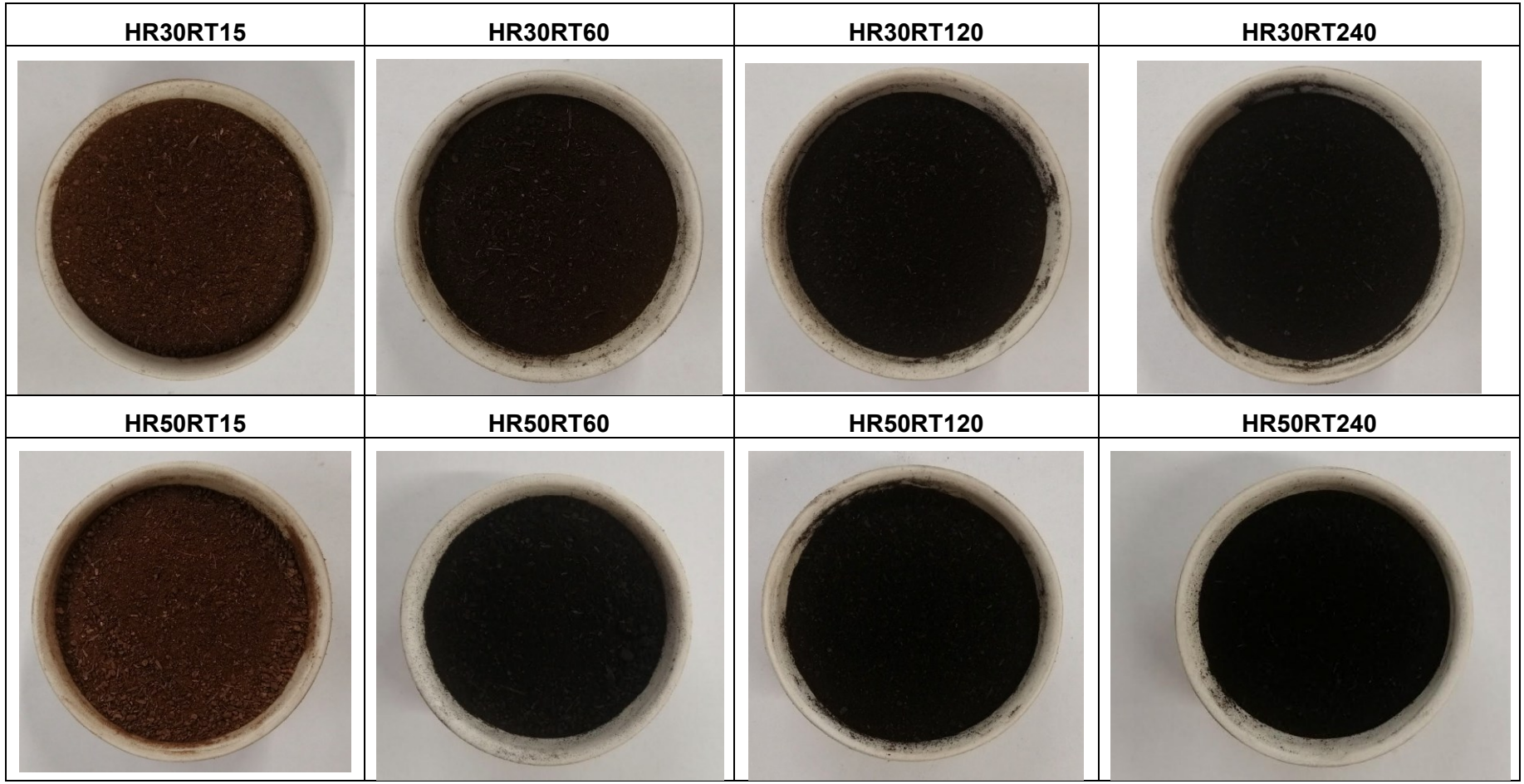

Fig. A3. Photographs of torrefied biomass depending on the production variant (photographs were taken in a crucible with a diameter of 40 mm)